Quaternary International 673 (2023) 1–17

Contents lists available at ScienceDirect

Quaternary International

journal homepage: www.elsevier.com/locate/quaint

Bioproductivity and vegetation changes documented in Eifel maar lake sediments (western Germany) compared with speleothem growth indicating three warm phases during the last glacial cycle

Dana F.C. Riechelmann [a,*], Johannes Albert [a], Sarah Britzius [a,b], Frederik Krebsbach [a], Denis Scholz [a], Fiona Schenk [a], Klaus Peter Jochum [b], Frank Sirocko [a]

[a] Institute for Geosciences, Johannes Gutenberg University Mainz, Johann-Joachim-Becher-Weg 21, 55128 Mainz, Germany
[b] Climate Geochemistry Department, Max Planck Institute for Chemistry, Hahn-Meitner-Weg 1, 55128 Mainz, Germany

ARTICLE INFO

Keywords:
Marker tephra layers
Organic carbon (chlorins)
Pollen assemblage
^{230}Th/U-dating
Eemian
Marine Isotope Stage 3

ABSTRACT

Understanding supra-regional climate variability such as the changes in the North Atlantic realm is important to identify the drivers of the climate system. In this study maar lake sediments from the Eifel (western Germany) were analysed with a multi-proxy approach and compared to central and western European speleothem growth phases.

C_{org} (chlorins) and the pollen assemblage were analysed from two sediment cores of the Hoher List infilled maar lake. To generate C_{org} (chlorins) and pollen records covering the entire last 130,000 yr b2k (years before year 2000 CE), the data from this study were stacked with published data from other Eifel maar lake sediment cores (Sirocko et al., 2013, 2021, 2022). The sediment cores from Hoher List infilled maar lake were dated by marker tephra layers giving chronological anchor points and the precise dating of the sediment cores was performed by the tuning of the C_{org} (chlorins) records to the NGRIP $\delta^{18}O$ record (Rasmussen et al., 2014). The speleothems, whose growth phases are compared to the lake sediment proxy records, were compiled from the literature as well as speleothems from Dechencave (western Germany) dated by the ^{230}Th/U-method in this study.

The C_{org} (chlorins) variability shows the bioproductivity in the maar lake, which is related to water temperature and corresponds to the Greenland Interstadials (GIs) in the NGRIP $\delta^{18}O$ record indicates its dependence on supra-regional climate variations in the North Atlantic. The pollen record shows three periods of forest with temperate forest species, during the Eemian, early Marine Isotope Stage (MIS) 3, and the Holocene. Speleothem growth in four caves in central and western Europe (Dechencave, Spannagel Cave, Hölloch Cave, Villars Cave) is predominantly sensitive to cold periods with glaciers and/or permafrost conditions above the caves inhibiting speleothem growth. The forested phases and phases of high bioproductivity in the Eifel correspond well with phases of speleothem growth indicating three warm phases in central Europe during the last glacial cycle.

1. Introduction

Climate proxy records covering the entire last glacial cycle from the Eemian to the Holocene are important to understand the climate variability from interglacial to glacial and *vice versa* as well as the millennial scale variations, such as Dansgaard/Oeschger (D/O) events (Dansgaard et al., 1993). The most prominent records for the northern hemisphere, in particular the North Atlantic realm, are available from Greenland ice cores, such as the NGRIP $\delta^{18}O$ record (North Greenland Ice Core Project, 2004; Rasmussen et al., 2014), and marine sediments, such as Atlantic sea surface temperature (e.g., Martrat et al., 2007). The North Atlantic realm is a sensitive region for these orbital and millennial scale climate changes, such as glacial-interglacial cycles, as well as changes on millennial scales, such as D/O-events, which are due to changes in the Atlantic Meridional Overturning Circulation (AMOC) (e.g., Böhm et al., 2015; Rahmstorf, 2002). These changes were identified for example in the C_{org} (chlorins) record from Eifel sediment cores for approximately the last 60,000 yr b2k (years before year 2000 CE; Sirocko et al., 2021),

* Corresponding author.
E-mail address: riechelm@uni-mainz.de (D.F.C. Riechelmann).

https://doi.org/10.1016/j.quaint.2023.11.001
Received 7 June 2023; Received in revised form 5 November 2023; Accepted 5 November 2023
Available online 15 November 2023

pollen (e.g., Britzius and Sirocko, 2023; Fletcher et al., 2010; Kern et al., 2022; Sirocko et al., 2022), diatom (e.g., Ampel et al., 2010), and chironomid records across Europe (e.g., Bolland et al., 2022; Engels et al., 2008b). In addition, proxy records of speleothems from different caves located in central and western Europe (e.g., Bunker Cave, Spannagel Cave, Hölloch Cave, Villars Cave) indicate D/O-events and changes of the North Atlantic Oscillation (NAO) during the Holocene (Fohlmeister et al., 2012; Genty et al., 2010; Moseley et al., 2020; Spötl and Mangini, 2002; Wassenburg et al., 2016; Weber et al., 2018). Therefore, central and western Europe, between the Fennoscandian and Alpine ice sheets, are an ideal region to study climate variability with different climate archives and multi-proxy approaches.

However, high resolution terrestrial climate archives from central and western Europe with proxy records covering this entire last glacial cycle are dominated by peat bogs and lake sediments and are still scarce as well as bearing the problem of absolute dating beyond the ^{14}C-dating range (Helmens, 2014). A possible dating method, which can be used for dating beyond the ^{14}C-dating range, is optically stimulated luminescence (OSL), however, providing relatively large uncertainties (e.g., Engels et al., 2008a; Helmens, 2014; Helmens and Engels, 2010). Depressions in the landscape filled by lakes or peat bogs in northern Europe and the Alps are generally formed by the ice of the glaciers and therefore contain sediments of the subsequent interglacial period (Helmens, 2014). They are potentially covered by ice during the next glacial period and do not provide continuous records over glacial-interglacial cycles (Sirocko et al., 2016). The Eifel maar lakes are ideal to preserve such records because they are not formed by glaciers but by volcanic eruptions and the Eifel was continuously ice free during the last 130,000 yr b2k (Ehlers et al., 2011). However, due to the frequent eruptions and siltation of the lakes, sediment cores from different maar lakes have to be stacked to continuous proxy records over glacial-interglacial cycles (Sirocko et al., 2005, 2016, 2021, 2022).

In this study, the published ELSA-20 stack of C_{org} (chlorins) (Sirocko et al., 2021) and pollen records (Sirocko et al., 2022) covering approximately the last 60,000 yr b2k are stacked to the C_{org} (chlorins) and pollen records of the cores HL2 and HL4, from the Hoher List infilled maar lake, covering the time back from approximately 60,000 to 130,000 yr b2k, determined in this study. In the study of Sirocko et al. (2005), the core HL2 was varve counted between 65 and 47.5 m and analysed for its quartz grains in the loess fraction as well as the loess and pollen content. From these data a late Eemian aridity pulse at 118,000 yr b2k was interpreted. In addition, the pollen record of core DE3 from infilled Dehner Maar (Sirocko et al., 2013, 2016) was partly added to the compilation of the other pollen records. Therefore, the stacking of these proxy records results in a continuous record covering the entire last glacial cycle.

Another terrestrial climate archive are speleothems, which cannot provide such continuous proxy records from central and western Europe due to speleothem growth being dependent on liquid water and CO_2 from soil and vegetation above the caves. These prerequisites for speleothem growth are not fulfilled during cold and dry periods in central and western Europe, such as glacial periods with glaciers or permafrost above the caves (e.g., Spötl and Mangini, 2007). However, they can be precisely and absolutely dated by the ^{230}Th/U-method (e.g., Scholz and Hoffmann, 2008). Therefore, phases of speleothem growth can be used as an independently dated proxy for warm and wet climate periods.

The goals of this study are: (i) constructing a robust chronology for the analysed sediment cores, (ii) extending the published records from the Eifel maar lakes of C_{org} (chlorins) (Sirocko et al., 2021) and pollen (Sirocko et al., 2022) for approximately the last 60,000 yr b2k back to the Eemian, (iii) comparison of the proxy records from the Eifel sediment cores with speleothem growth phases of three speleothems from Dechencave, which were precisely determined in this study, and compiled speleothem growth phases from the literature from four central and western European caves, and (iv) comparison of the resulting pollen record to other central and western European pollen records for the last 130,000 yr b2k.

2. Material and methods

2.1. Sampling sites

2.1.1. The site of the Hoher List (HL) infilled maar sediment cores

The Hoher List infilled maar lake (50°10′ N, 6°51′ E) is located 1.8 km west of Schalkenmehren in the west Eifel volcanic field in western Germany (Fig. 1) (Sirocko et al., 2013). Two sediment cores, HL2 and HL4, were investigated in this study and were drilled from this infilled maar lake (Fig. 1b) in the framework of the ELSA Project (Eifel Laminated Sediment Archive) of the Institute for Geosciences at the Johannes Gutenberg University Mainz (Germany) (Sirocko et al., 2013). Core HL2 has a length of 104 m (Fig. 2a) and was drilled on the flank of the crater (Fig. 1b) in 2003 CE. Core HL4 has a length of 62 m (Fig. 2b) and was drilled in 2006 CE. Due to several coarse-grained sections from slumps in core HL2 (Fig. 2a), core HL4 was drilled in 100 m distance from HL2, located in the centre of the infilled maar structure (Fig. 1b). The comparison of both cores reveals that HL2 was apparently affected by processes of sediment reworking at the former lake flanks and HL4 is better laminated/varved and thus represents the sedimentation processes in the centre of the maar lake (Fig. 2a and b).

2.1.2. The site of the infilled Dehner Maar (DE) sediment core

The infilled Dehner Maar (50°17′ N, 6°30′ E), near the town Reuth, is located 29 km northwest of the Hoher List infilled maar. The core DE3 has a length of 88 m and the lowermost meter of the core is the volcanic sediment (tephra) of the eruption of this maar (Fig. 2c). In this study, the pollen record of core DE3 from 83.6 to 76.4 m was used to fill the gap in the pollen record in the upper part of the two HL cores, where pollen are not preserved (see section 2.4). The pollen record of the entire core DE3 for 85 m is published in Sirocko et al. (2013). For further details of this core, see Sirocko et al. (2016).

2.2. Tephra analyses

The tephra deposits can be recognized in the cores by an abrupt change in grain size from clay to silt or sand, accompanied by a change in colour to dark greyish with light and dark sections (indicated in red in Fig. 2). Förster and Sirocko (2016) defined ten different minerals and rock fragments, which are sufficient to characterise a tephra, which are amphiboles, pyroxenes, scoria + pumice, sanidine, leucite, and mica for the volcanogenic fraction. This is modified in this study whereat leucite and pumice are not included, leucite due to its rare occurrence and pumice due to its hydroplane characteristic bearing problems during wet sieving. In addition, reddish and greyish sandstone as well as quartz are used in the study of Förster and Sirocko (2016) to relate the eruption to the regional geology, which is an important additional information to distinguish phreatomagmatic maar eruptions from pure volcanic eruptions and to relate the tephra to a volcano or maar. In this study quartz was excluded, due to that it is also a frequent mineral in the normal sedimentation in the maar lakes and not only occurring in the tephra layers. The prerequisites for marker tephra layers are (i) visual identification in sediment cores from at least two different maar sites, (ii) a thickness of $\geq$1 cm, and (iii) a characteristic petrographic composition (c.f., Förster and Sirocko, 2016). Accordingly, the marker tephra layers do not represent the full record of volcanic activity in the Eifel but only show the clearly recognisable marker tephra layers, which can be correlate to each other.

As the mineral composition can change during fallout, the whole event-layers in their entire thickness were sampled. Sample material was taken from each tephra layer, wet sieved for the fraction 125–250 μm and dried. A representative fraction of each sample was visually analysed under a binocular microscope VisiScope 260 SZB260 (*VWR, Darmstadt, Germany*) with 15–45× magnification. At least 100 mineral

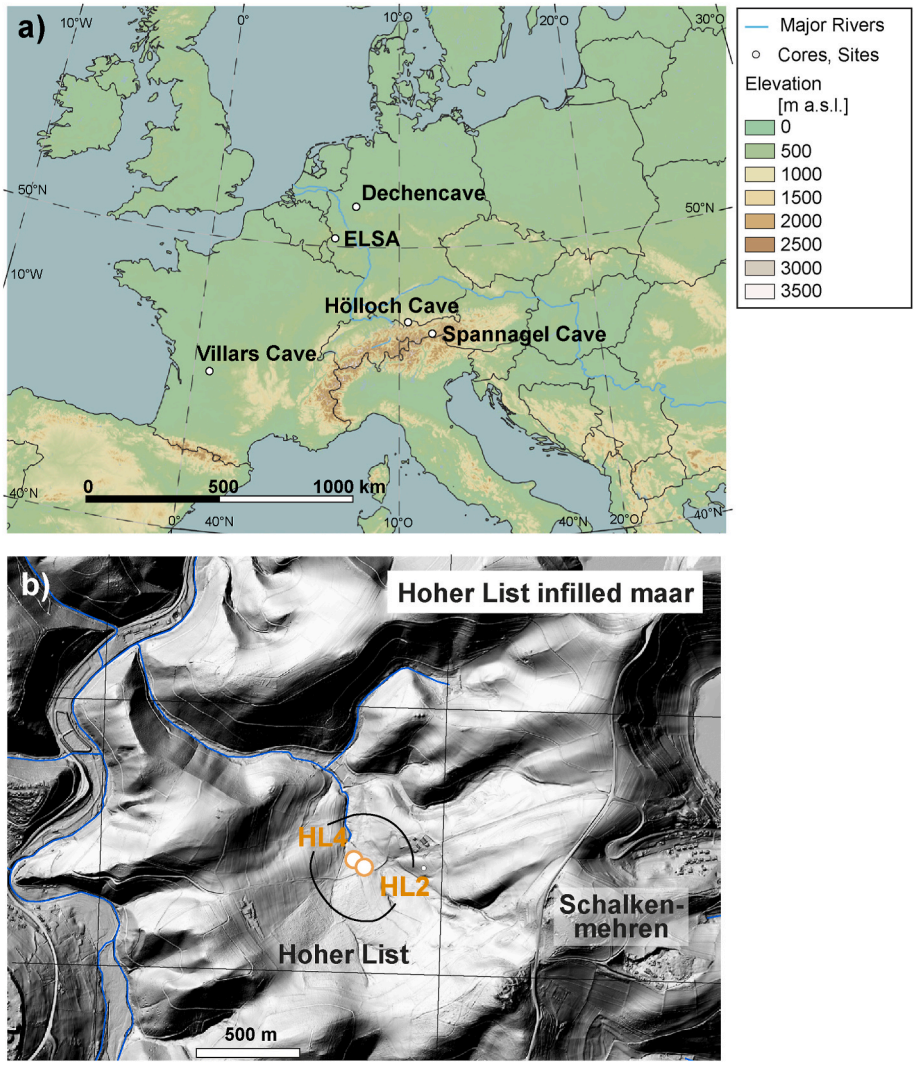

Fig. 1. a) Topographical map of central and western Europe indicating sediment core sampling site (ELSA) in the Eifel and the four cave locations. b) Digital elevation model of the modern topography of the Hoher List infilled maar with indication of the drilling locations of the two cores (HL2, HL4).

grains were determined, counted, and then used to calculate the petrographic histograms for the different marker tephra layers (Fig. 3). This approach enables to characterise a marker tephra layers for the correlation between cores and relate them to a volcano or maar eruption.

2.3. C_{org} (chlorins) analysis

The C_{org} (chlorins) time series for both cores HL2 and HL4 were analysed by the In Situ Reflectance Spectroscopy (ISRS) method with a Gretag Spectrolino instrument (*GretagMacbeth, Regensdorf, Switzerland*). The resolution of the measurements were 2 mm increments for core HL2 and 1 mm increments for core HL4. This instrument measures the reflectance for each wavelength of the visible light with a spectral resolution of 10 nm relative to a white colour standard given in percent. The method was developed by Rein and Sirocko (2002) and further improved by Sirocko et al. (2021) and uses the spectral characteristic of the absorption of chlorophyll and its degradation products around 670 nm to determine the chlorins content. C_{org} (chlorins) does not represent the total organic carbon in the sediment, which would include plant debris, but only the chlorophyll from algae and bacteria. In case of the Hoher List infilled maar, this mainly consists of chlorophyll from diatoms and chrysophytes, representing the aquatic bioproductivity in the lake. A detailed description of the method is presented in Sirocko et al. (2021).

2.4. Pollen analysis

Pollen preparation was done according to Berglund and Ralska-Jasiewiczowa (1986) and Faegri and Iversen (1989). Pollen samples span a depth range of 1 cm and have a volume of about 1 cm^3. The sample resolution for HL2 is 1–70 cm, 1–160 cm for HL4, and 2–21 cm for the part from 83.6 to 76.4 m depth of core DE3 used in this study. Samples were treated with potassium hydroxide solution (KOH), hydrochloric acid (HCl), and hydrofluoric acid (HF). For acetolysis, acetic acid ($C_2H_4O_2$) and a mixture (9:1) of acetic anhydride ($C_4H_6O_3$) and sulfuric acid (H_2SO_4) were used. Centrifugation was done at 3000–3500 rpm for 5 min. The samples were sieved at 200 μm and afterwards filtered at 10 μm. The samples were mounted on microscope slides with anhydrous glycerol ($C_3H_8O_3$). Pollen were counted with a VisiScope BL 114 (*VWR, Darmstadt, Germany*) under a maximum of six-hundred-fold magnification. Whenever possible, 300 pollen grains were counted for each sample. Percentages (% of all terrestrial pollen) are presented only for those samples where the sum of all taxa exceeds at minimum 50 pollen grains. Samples with lower counts are statistically not robust and, therefore, not shown in the stack record. Pollen assemblages for the three single cores (HL2, HL4, DE3) showing all pollen counts are presented in the Supplement (Figs. S1, S2, and S3).

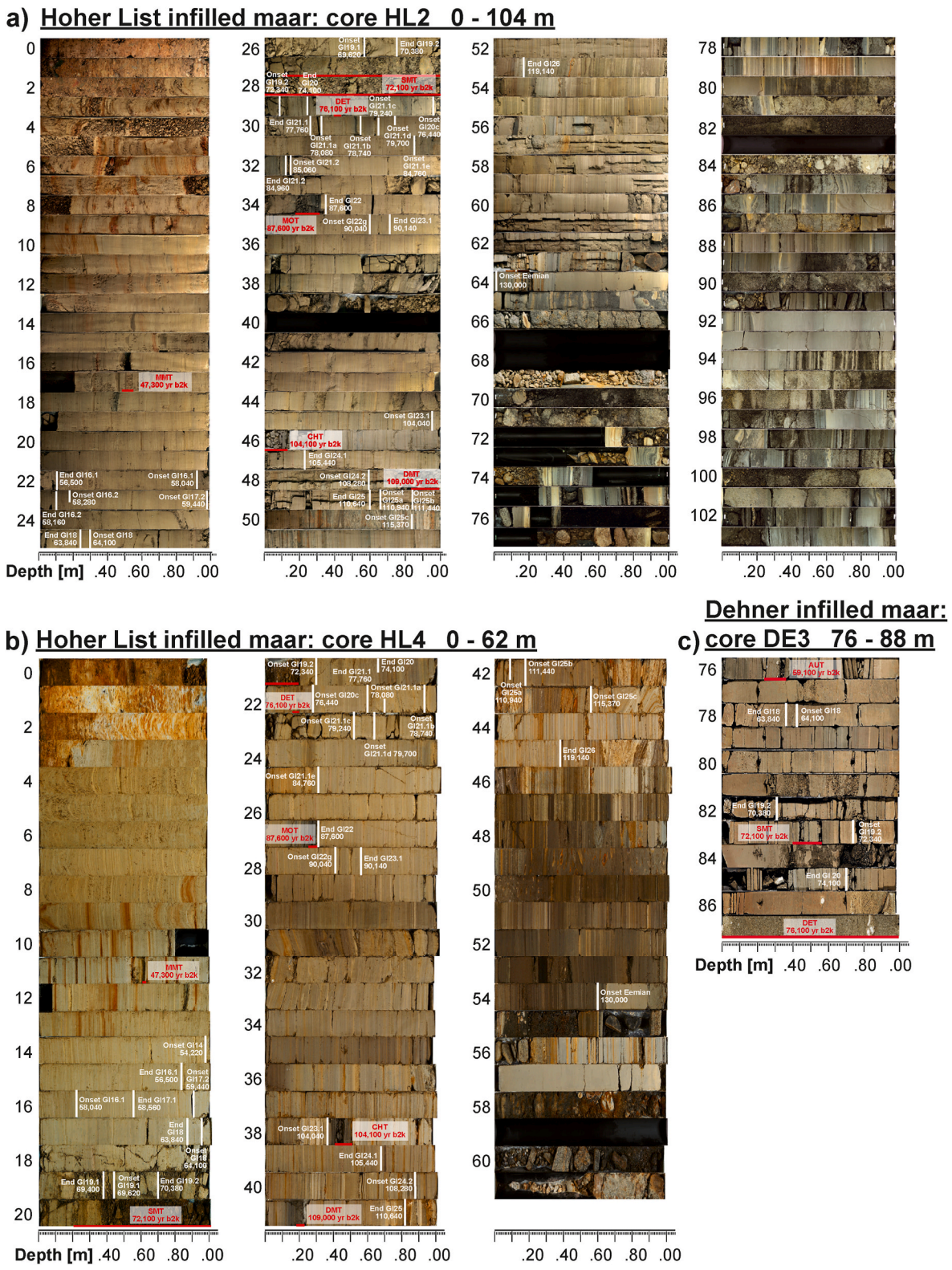

Fig. 2. Pictures of the sediment cores HL2 (a) and HL4 (b), and DE3 from 76 to 88 m (c) with indication of the maker tephra layers in red and the onsets and ends of the Greenland Interstadials (GIs) in white.

Furthermore, it has to be taken into account that in core HL4, pollen were not preserved above the Schalkenmehrener Maar Tephra (SMT, 21.2 m) (Fig. 2b and S2). In addition, core HL2 shows sections without pollen between 34.8 and 32.6 m and above the SMT in 29.0 m (Fig. 2a and S1). This is probably related to a drop of the lake level and no anoxic conditions at the lake bottom (Fig. 4b). Therefore, this time span has to be filled by another pollen record to create a continuous record over the last 130,000 yr b2k. To cover the entire time span, the pollen record of the ELSA-20 stack covering the last 59,100 yr b2k (Sirocko et al., 2022), the core DE3 from infilled Dehner Maar (see section 2.1.2, Fig. S3)

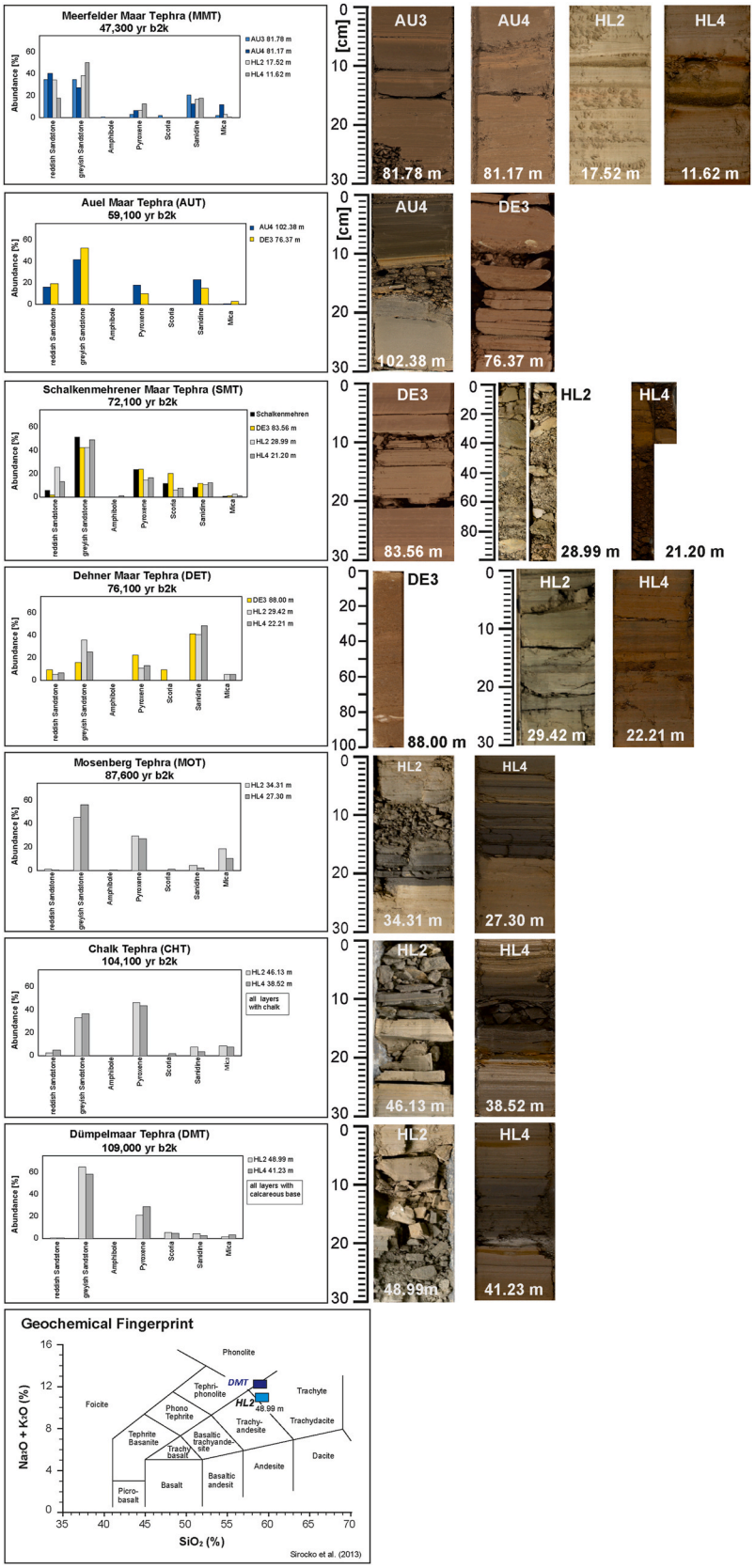

Fig. 3. The seven marker tephra layers are present with their typical mineral distribution shown as histograms on the left side. On the right side, pictures of the corresponding seven marker tephra layers are shown from the cores HL2, HL4, and DE3 as well as AU3 and AU4 of Auel Maar for comparison (Sirocko et al., 2021). The depth indicated in the pictures gives the base depth in the cores for the different marker tephra layers. In the lowermost panel, the anchor tephra from the Dümpelmaar (DMT) is shown with its geochemical fingerprint and the distinct relation of this tephra in the HL2 core to the Dümpelmaar eruption (Sirocko et al., 2013).

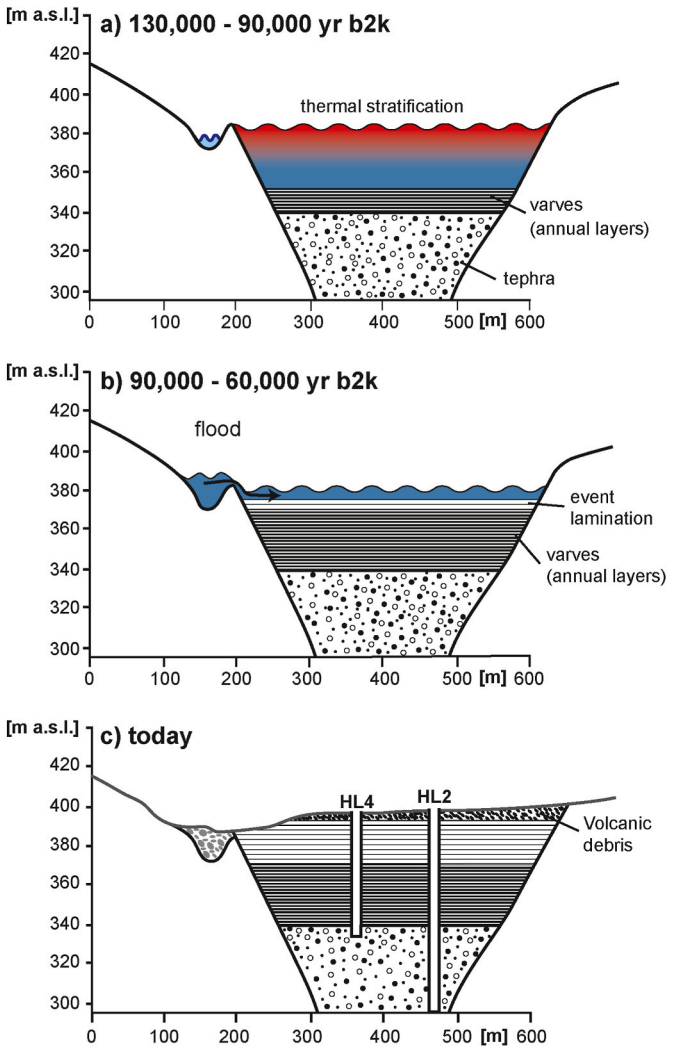

Fig. 4. Schematic depth transects through the Hoher List maar lake and infilled maar structure showing the different sedimentation regimes during 130,000–90,000 yr b2k (a), 90,000–60,000 yr b2k (b), and today (c).

(Sirocko et al., 2013, 2016), covering the time span from 72,100 to 59,100 yr b2k, and the composite of the two HL cores, covering the time span from 130,000 to 72,100 yr b2k, were stacked.

The comparison with other central and western European pollen records is based on the tree pollen vs. non-tree pollen ratio, which was calculated as follows for all data series:

$$\left(\frac{\frac{\text{Total AP}}{\text{Total NAP}}}{\left(\frac{\text{Total AP}}{\text{Total NAP}}\right)_{max}}\right)*100 \quad (1)$$

Whereas AP includes all arboreal pollen (*Abies*, *Picea*, *Pinus*, *Betula*, *Alnus*, *Corylus*, *Carpinus*, *Quercus*, *Tilia*, *Ulmus*, *Fraxinus*, *Fagus*, *Taxus*, *Salix*, *Juniperus*, *Juglans*), NAP includes all non-arboreal terrestrial pollen (Poaceae, Ericaceae, *Artemisia*, Caryophyllaceae, Chenopodiaceae, Ranunculaceae, Apiaceae, *Tubuliflorae*, *Liguliflorae*, Cerealia, *Secale*, *Fagopyrum*, Plantaginaceae, *Hedera*, *Viscum*).

2.5. Speleothem dating and age compilation

The prerequisite for speleothem growth is liquid water and CO_2 from vegetation and soil, which produces carbonic acid eventually dissolving the carbonate host rock. The seeping water supersaturated with calcium carbonate then forms speleothems in the cave. Therefore, speleothems cannot grow when it is too cold or dry. For example, under permafrost conditions, there will be no liquid water dripping into the cave, and speleothems cannot grow. Furthermore, cold and dry conditions result in less or even no vegetation and/or formation of soil, which leads to no or too little CO_2 production to dissolve the host rock. Therefore, the drip water will not be supersaturated with respect to calcium carbonate (Fairchild and Baker, 2012). Due to these circumstances, speleothem growth at itself can be used as a climate proxy detecting times of warm and wet climate, such as interglacial periods. However, speleothem growth can also stop due to cave or drip site specific reasons and not only cold and dry climate, which is known from several caves (e.g., Fohlmeister et al., 2012; Genty et al., 2003; Spötl et al., 2007; Weber et al., 2021). Therefore, in order to relate phases without growth to climate, several stalagmites from a cave should be dated (e.g., Spötl and Mangini, 2007). Thus, the following criteria were taken as a basis to select cave systems from the literature whose speleothem growth phases were compared to the proxy records from the Eifel sediment cores: (i) the cave site has to be located in central or western Europe (Fig. 1a), (ii) more than five stalagmites have to be dated from each cave, and (iii) these dated stalagmites have to spread over the time span of the last 130,000 yr b2k. This results in four cave sites in total. First cave site is the cave system containing Bunker Cave (three stalagmites, one flowstone), B7-Cave (three stalagmites), Hüttenbläserschacht Cave (four stalagmites), and Dechencave (this study, see below). Stalagmites from the Holocene were dated from Bunker Cave (Fohlmeister et al., 2012; Waltgenbach et al., 2020, 2021), Hüttenbläserschacht Cave (Weber et al., 2021), and B7-Cave (Niggemann et al., 2003; Riechelmann et al., 2023). A stalagmite from the MIS 3 was dated from Bunker Cave (Weber et al., 2018) as well as newly dated samples from Dechencave presented in this study spread over the time back to 130,000 yr b2k. The other three cave sites from the literature are Spannagel Cave (47°05′ N, 11°40′ E; 2500 m asl) (including Kleegruben Cave (10 stalagmites, 1 flowstone); Spötl et al., 2006a) in the Austrian Alps (Spötl et al., 2002), Hölloch Cave (8 stalagmites; 47°23′ N, 10°09′ E; 1440 m asl) in the German/Austrian Alps (Wurth et al., 2004), and Villars Cave (6 stalagmites, 1 flowstone; 45°27′ N, 0°48′ E; 175 m asl) in western France (Genty et al., 2002) (Fig. 1a).

Dechencave (51°22′ N, 7°29′ E; 170 m asl) is located at the northern edge of the Rhenish Slate Mountains in western Germany (Fig. 1a) and it is part of a large cave system in the Grüne Valley in the Sauerland. To this cave system also belongs Bunker Cave, which was intensively investigated in the last decade for its speleothems and during cave monitoring studies (e.g., Fohlmeister et al., 2012; Riechelmann et al., 2022; Riechelmann et al., 2011; Weber et al., 2018). Furthermore, Hüttenbläserschacht Cave and B7-Cave belong to this cave system from which also speleothems were investigated (Niggemann et al., 2003; Riechelmann et al., 2023; Weber et al., 2021). This cave system is the most intensively investigated one nearest to the Eifel.

Two stalagmites and one flowstone (DH_Kn5, DH_Kn6, DH_Kn7) were sampled from an excavation in the Dechencave. In this study, samples of approximately 300 mg were drilled with a hand-held drill from these speleothems for ^{230}Th/U-dating and these powder samples were dissolved in 7 N HNO_3. A mixed ^{229}Th–^{233}U–^{236}U spike was added (see Gibert et al. (2016) for details on spike calibration) and afterwards the U and Th factions were separated by ion-exchange column chemistry (Yang et al., 2015). The samples were analysed using a Nu plasma multi collector-inductively coupled plasma (MC-ICP) mass spectrometer (*Nu Instruments Ltd., Wrexham, UK*) at the Max Planck Institute for Chemistry (Mainz) (20 samples) and a Neptune plus MC-ICP mass spectrometer (*Thermo Scientific, Bremen, Germany*) at the Institute for Geosciences, Mainz University (one sample). For details of the MC-ICP-MS measurements, see Obert et al. (2016).

3. Results

3.1. Sedimentation processes in the Hoher List maar lake

Fig. 4 shows a schematic depth transect through the Hoher List maar lake and infilled maar structure, outlining the sedimentation processes in the lake after the eruption just before the beginning of the Eemian (Förster and Sirocko, 2016). The lowermost 38 m of core HL2 and 7.4 m of core HL4, respectively, are represented by volcanic sediments (tephra) from the maar's eruption (Fig. 2a and b, and 4). After the formation of a lake in the crater with a thermal stratification and a continuous outflow of the lake water into the adjacent creeks, the sediments were deposited as varves (Fig. 4a). This sedimentation pattern changed around 90,000 yr b2k, when the climate became colder and dryer, and the lake level apparently dropped as well as lake water depth due to the continuously filling of the lake with sediments. This water level change is documented in the layering of the sediments, which changed from continuous mm-thick annual varves to a sedimentation dominated by cm-thick flood event layers (Fig. 4b). The digital elevation model of the modern topography shows that the former lake was touched by several creeks, today deeply incised into the landscape (Fig. 1b). Flash floods (summer rain or winter meltwater events) most probably transported fine-grained sediments into the adjacent lake, causing many of the thin, whitish event layers, which mark seasonal flood layers (Fig. 2a and b). From approximately 60,000 yr b2k until today the lake was silted up as well as coarse-grained volcanic debris from the crater flanks was reworked and filled up the crater structure, representing the uppermost 5.3 m in core HL2 and 3.2 m in core HL4 (Fig. 2a, b, and 4c).

In the upper 18 m of core HL2 the C_{org} (chlorins) was not preserved as well as in the uppermost 13 m of core HL4 i.e., the phase of silting up of the lake. In these parts of the cores, C_{org} (chlorins) is not preserved because of groundwater influence, providing oxic conditions visible in the reddish layers in the cores, resulting from the siltation of the lake (Fig. 2a and b).

3.2. Chronology

Marker tephra layers are important for the dating of the HL2, HL4, and DE3 sediment cores because they are beyond the ^{14}C-dating range of approximately 55,000 yr b2k (Hajdas et al., 2021). In the sediment cores HL2 and HL4, six marker tephra layers can be identified, and three marker tephra layers in the lower part of the DE3 sediment core used in this study by the above-mentioned criteria, which were used to correlate the cores to each other. These tephra layers are from the eruptions of the Dümpelmaar (DMT, oldest tephra in the HL cores), Chalk Tephra (CHT, unknown origin), Mosenberg (MOT), Dehner Maar (DET, own eruption in DE3 core), Schalkenmehrener Maar (SMT, nearest eruption in the HL cores), Auel Maar (AUT, only in core DE3), and Meerfelder Maar (MMT, youngest tephra in the HL cores) (Figs. 2 and 3, and Table 1). These tephra layers are identified by their specific petrographic composition. Ages of the marker tephra layers were obtained using the dated eruption ages of DMT, MOT, AUT, and MMT (Leyk and Lippoldt, 1997; Schaber and Sirocko, 2005; Sirocko et al., 2021; van den Bogaard et al., 1989) and the tuning of the C_{org} (chlorins) records of the two HL cores to the NGRIP δ^{18}O record (Rasmussen et al., 2014) stadial/interstadial succession (see section 3.3, Fig. 5, and Table 2).

The DMT is characterised by around 60% of greyish sandstone and more than 20% of pyroxene, giving a trachytic geochemical composition (Fig. 3) (Förster et al., 2020; Sirocko et al., 2013). This phreatomagmatic eruption was dated by van den Bogaard et al. (1989) by the ^{40}Ar/^{39}Ar method to $\leq$ 116,000 ± 16,000 yr b2k (Table 1). The varve counting between 132,000 and 106,000 yr b2k and grey scale - NGRIP δ^{18}O record tuning by Sirocko et al. (2005) of the HL2 core indicate an age of 105,000 yr b2k for the DMT. This is in line with the C_{org} (chlorins) HL - NGRIP δ^{18}O record tuning, dating this tephra in this study to 109,000 yr b2k (Fig. 5c, Table 2).

The next marker tephra is characterised by 50% of pyroxenes and 30% of greyish sandstone (Fig. 3), associated with carbonate from lake chalk. The volcano of this eruption is unknown. However, the typical chalk content in this tephra (Fig. 3, Table 1) was also identified in sediment cores from other maar lakes (Sirocko et al. in prep.). The lake chalk is not related to the erupted material but formed during the sedimentation of the tephra in the lakes from calcium carbonate produced by microorganisms. This lake chalk in association with pyroxenes is a unique feature of all tephra layers in all ELSA cores and therefore named Chalk Tephra (CHT). Due to the relation to productive microorganisms, the chalk indicates rather warm climatic conditions, which matches the C_{org} (chlorins) HL - NGRIP δ^{18}O record tuning, dating this tephra at the onset of Greenland Interstadial (GI) 23 with an age of 104,100 yr b2k (Fig. 5c, Table 2).

The petrographic composition of the next marker tephra with 50% greyish sandstone, 30% pyroxenes, and 10% mica (Fig. 3) is geochemically identified by its pyroxenes as the MOT (Förster et al., 2020). The MOT has been dated by different methods (thermoluminescence, OSL, ^{40}Ar/^{39}Ar) between 87,000 and 42,000 yr b2k and concluded to an approximate age of 80,000 yr b2k for the Mosenberg eruption and a younger eruption phase around 50,000 to 40,000 yr b2k including the Meerfelder Maar (Sirocko et al., 2013; and references therein). ^{40}Ar/^{39}Ar dating results in an age of 81,000 ± 23,000 yr b2k for the

Table 1
Compilation of the characteristics, depths in cores, absolute and tuned ages of the seven marker tephra layers. Tephra only occurring in core DE3 is written in italics.

Marker tephra layers	Petrographic composition	Depth in cores (HL2/HL4)	Ages (yr b2k) derived from the literature	Age (yr b2k) tuned to NGRIP δ^{18}O record (Rasmussen et al., 2014) in this study
Meerfelder Maar Tephra (MMT)	70% greyish and reddish sandstone	17.52–17.51 m/ 11.62–11.61 m	45,900 + 1200/−1040 Schaber and Sirocko (2005) (^{14}C-dating) 47,300 ± 1945 (Sirocko et al., 2021) tuning C_{org} (chlorins) to NGRIP δ^{18}O record	–
Auel Maar Tephra (AUT)	40% greyish sandstone 10% Pyroxene 10% Sanidine	*76.37-76.24 m (DE3)*	*59,100 ± 2560 Sirocko et al. (2021) tuning C_{org}(chlorins) to NGRIP δ^{18}O record*	–
Schalkenmehrener Maar Tephra (SMT)	20% Pyroxene 10% Sanidine 10% Scoria	28.99–27.10 m/ 21.20–20.21 m	–	72,100 ± > 2573
Dehner Maar Tephra (DET)	40% Sanidine	29.42–29.41 m/ 22.21–22.19 m	–	76,100 ± > 2573
Mosenberg Tephra (MOT)	Foicite	34.31–34.26 m/ 27.30–27.26 m	81,000 ± 23,000 Leyk and Lippoldt (1997) (^{40}Ar/^{39}Ar dating)	87,600 ± > 2573
Chalk Tephra (CHT)	Containing Lake Chalk	46.13–46.00 m/ 38.52–38.41 m	–	104,100 ± > 2573
Dümpelmaar Tephra (DMT)	Trachyte	48.99–48.83 m/ 41.23–41.18 m	≤116,000 ± 16,000 van den Bogaard et al. (1989) (^{40}Ar/^{39}Ar dating)	109,000 ± > 2573

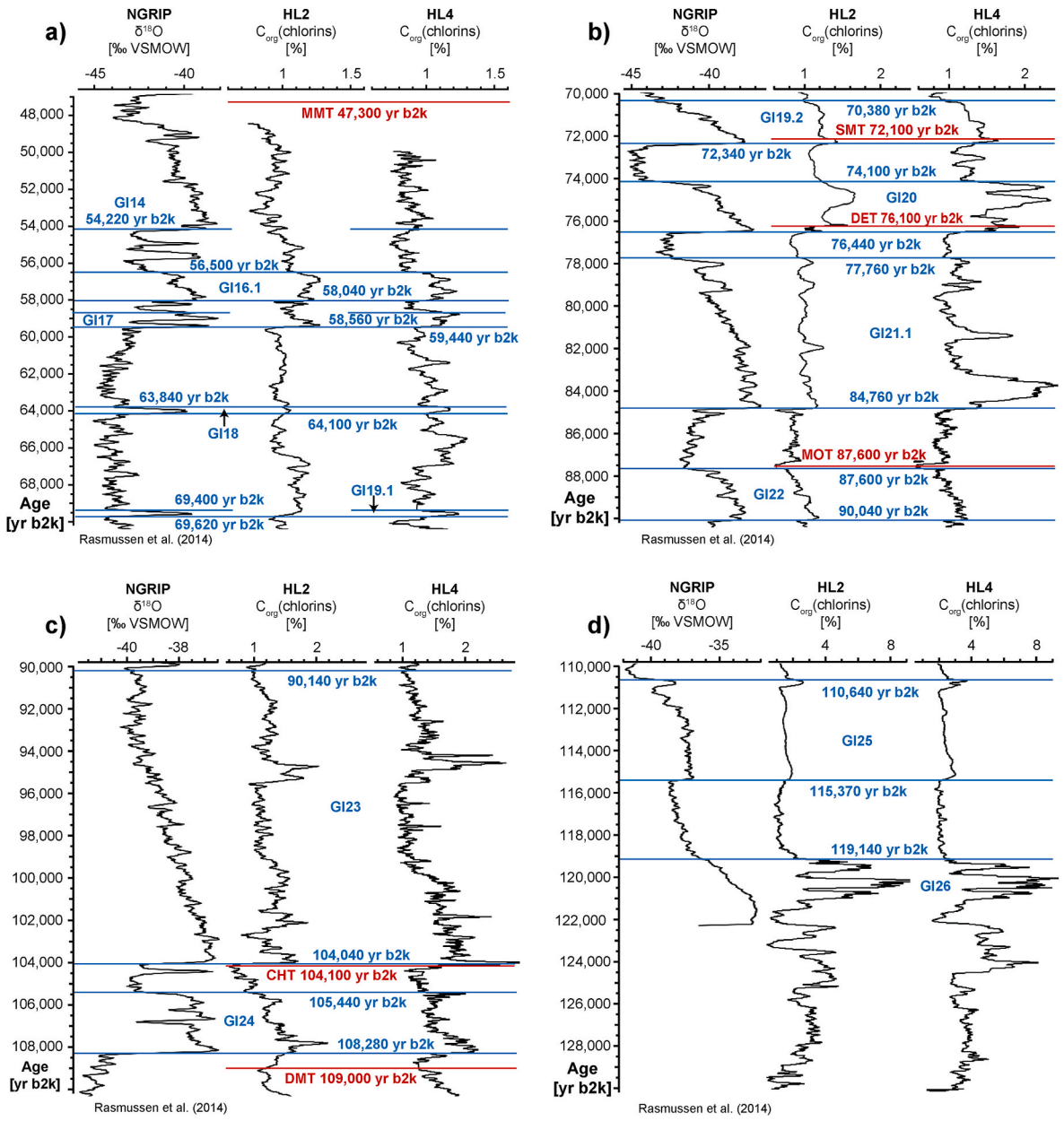

Fig. 5. The $\delta^{18}O$ record from the NGRIP ice core (North Greenland Ice Core Project, 2004; Rasmussen et al., 2014) is the reference record to which the C_{org} (chlorins) records of HL2 and HL4 are visually tuned. The marker tephra layers are indicated in red with their tuned ages, as well as the onsets and ends of the GIs (blue lines) which are given by the NGRIP $\delta^{18}O$ record (Rasmussen et al., 2014). 70,000 to 47,000 yr b2k are shown in (a), 90,000 to 70,000 yr b2k in (b), 110,000 to 90,000 yr b2k in (c), and 130,000 to 110,000 yr b2k in (d).

MOT (Leyk and Lippoldt, 1997) (Table 1). The age determined in this study by the C_{org} (chlorins) HL - NGRIP $\delta^{18}O$ record tuning is 87,600 yr b2k (Fig. 5b, Table 2), which is in agreement with the $^{40}Ar/^{39}Ar$ dating.

The mineral composition of the DET is distinguished by 40% of sanidine (Fig. 3, Table 1). The C_{org} (chlorins) HL - NGRIP $\delta^{18}O$ record tuning in this study results in an age of 76,100 yr b2k for the DET (Fig. 5b, Table 2).

The SMT contains 20% pyroxenes, 10% scoria, and 10% sanidines as well as 40% of greyish sandstone (Fig. 3, Table 1). This petrographic composition is known only from the tuff wall of the Schalkenmehrener Maar lake, and can thus be faithfully related to this eruption as well as by its geochemical composition (Förster et al., 2020). Furthermore, it is the thickest tephra deposit in the two HL cores (Fig. 2a and b, and 3), due to the nearby location of Schalkenmehrener Maar to the Hoher List infilled maar (Fig. 1b). Its age according to the C_{org} (chlorins) HL - NGRIP $\delta^{18}O$ record tuning in this study is 72,100 yr b2k (Fig. 5b, Table 2).

The AUT is assigned only in the DE3 core by roughly 40% of total mineral composition consisting of greyish sandstone as well as pyroxene and sanidine each abundant with 10% (Fig. 3). Furthermore, the AUT is the anchor tephra to combine the pollen record of the DE3 core to the ELSA-20 stack, which covers the time span from 59,100 yr b2k until present (Sirocko et al., 2021) (Fig. 6). The dating of the ELSA-20 stack was done by ^{14}C-dating of organic material in the sediment cores, as well as tuning of the C_{org} (chlorins) record to the NGRIP $\delta^{18}O$ record, resulting in the age of 59,100 yr b2k for the AUT (Sirocko et al., 2021).

The MMT is the youngest tephra in both HL cores and characterised by roughly 30–40% of total mineral composition consisting of greyish and reddish sandstone (Sirocko et al. in prep.) (Fig. 3, Table 1). Furthermore, the MMT is the anchor tephra to combine the HL cores to the ELSA-20 stack (Sirocko et al., 2021). The tuning of the ELSA-20 stack

Table 2
C_{org} (chlorins) tuned time markers (blue lines in Fig. 5) of cores HL2 and HL4 to the NGRIP $\delta^{18}O$ record Greenland Interstadial (GI) succession (North Greenland Ice Core Project, 2004; Rasmussen et al., 2014).

Time marker	[yr b2k]	HL2 [m]	HL4 [m]
MMT top		17.51	11.61
MMT base	**47,300**	17.52	11.62
Onset GI14	**54,220**		14.98
End GI16.1	**56,500**	22.10	15.84
Onset GI16.1	**58,040**	22.92	16.32
End GI16.2	**58,160**	23.10	
Onset GI16.2	**58,280**	23.18	
End GI17.1	**58,560**		16.56
Onset GI17.2	**59,440**	23.98	16.91
End GI18	**63,840**	25.24	17.88
Onset GI18	**64,100**	25.30	17.95
End GI19.1	**69,400**		19.38
Onset GI19.1	**69,620**	26.57	19.44
End GI19.2	**70,380**	26.74	19.70
SMT top		27.10	20.21
SMT base	**72,100**	28.99	21.20
Onset GI19.2	**72,340**	29.09	21.30
End GI20	**74,100**	29.24	21.66
DET top		29.41	22.19
DET base	**76,100**	29.42	22.21
Onset GI20c	**76,440**	29.96	22.28
End GI21.1	**77,760**	30.26	22.60
Onset GI21.1a	**78,080**	30.33	22.70
Onset GI21.1 b	**78,740**	30.55	22.93
Onset GI21.1c	**79,240**	30.65	23.52
Onset GI21.1 d	**79,700**	30.74	23.64
Onset GI21.1e	**84,760**	31.85	25.31
End GI21.2	**84,960**	32.12	
Onset GI21.2	**85,060**	32.15	
MOT top		34.26	27.26
MOT base	**87,600**	34.31	27.30
End GI22	**87,600**	34.35	27.31
Onset GI22g	**90,040**	35.60	28.41
End GI23.1	**90,140**	35.71	28.56
Onset GI23.1	**104,040**	45.95	38.37
CHT top		46.00	38.41
CHT base	**104,100**	46.13	38.52
End GI24.1	**105,440**	47.23	39.68
Onset GI24.2	**108,280**	48.59	40.88
DMT top		48.83	41.18
DMT base	**109,000**	48.99	41.23
End GI25	**110,640**	49.60	41.82
Onset GI25a	**110,940**	49.66	42.09
Onset GI25b	**111,440**	49.84	42.18
Onset GI25c	**115,370**	50.84	43.56
End GI26	**119,140**	53.17	45.38
Onset Eemian	**130,000**	64.00	54.60

C_{org} (chlorins) record to the NGRIP $\delta^{18}O$ record, resulting in the age of 47,300 yr b2k for the MMT (Sirocko et al., 2021) (Table 2). This fits with the ^{14}C-dating of organic material from this tephra of 45,900 + 1200/−1040 yr b2k (Schaber and Sirocko, 2005). Furthermore, this tephra was dated by thermoluminescence to 42,000 ± 3000 yr b2k (Zöller, 1989) and by OSL to 53,100 ± 1830 yr b2k (Zöller and Blanchard, 2009). All these ages are within agreement.

Furthermore, two InfraRed Radio Fluorescence (IR-RF) ages on K-feldspar of 88,000 ± 10,000 yr b2k in the depths of 42.30–42.15 m and 107,000 ± 20,000 yr b2k in the depths of 53.78–53.31 m in the HL2 core (Degering and Krbetschek, 2007) fits within their errors to the tuned ages of the GIs (indicated in white in Fig. 2a, Table 2) and are a good addition to confirm the chronology of the sediment cores. In conclusion, all ages enable to relate the pollen records from the two HL cores and the lower part of the DE3 core to an age (Fig. 6) and produce a reliable chronology.

3.3. C_{org} (chlorins) records

Greenland interstadials (GI) 26, GI 24, GI 23, GI 21, GI 20, GI 19, GI 17, and GI 16 are clearly visible as sharp increases in the C_{org} (chlorins) data of the two HL cores. GI 25, GI 22, GI 18, and GI 14 were identified as well, but do not show as sharp increases in the C_{org} (chlorins) as the aforementioned GIs (Fig. 5). In addition, the ELSA-20 stack shows more pronounced GIs in the C_{org} (chlorins) record than the C_{org} (chlorins) records of the two HL cores. This is due to the catchment of the river flowing through the Auel Maar lake, which provides a quite high amount of nutrients, having a positive effect on the bioproductivity in the lake (Sirocko et al., 2022). The Hoher List maar lake did not have an inflowing river. Therefore, the catchment of the lake is much smaller than for the Auel Maar and is just the crater structure (Fig. 1b) which provides less nutrients. This results in the general lower C_{org} (chlorins) and the not so pronounced GIs in the records of the two HL cores (Fig. 6). However, the C_{org} (chlorins) content of the lake sediments of cores HL2 and HL4 matches well with the NGRIP $\delta^{18}O$ record (Fig. 5), which is one of the most established records of the northern hemisphere climate (Rasmussen et al., 2014), showing almost all interstadial periods. Therefore, C_{org} (chlorins) records were visually age-tuned to the stadial/interstadial succession of the NGRIP ice core (North Greenland Ice Core Project, 2004; Rasmussen et al., 2014) from GI 26 to GI 14 using the independently dated marker tephra layers from Dümpelmaar eruption (DMT; van den Bogaard et al., 1989), Mosenberg eruption (MOT; Leyk and Lippoldt, 1997), and Meerfelder Maar eruption (MMT; Sirocko et al., 2021) as anchor points (see section 3.2). This tuning method is described in detail in Sirocko et al. (2016, 2021). A detailed overview of identified interstadials and sub-interstadials is presented in Table 2. Between these identified time markers from tephra layers as well as GI onsets and ends (Table 2), the ages were assigned by linear interpolation (Fig. S4). Overall, during the Eemian (MIS 5e), early MIS 3, and the last 14,000 yr b2k, both HL cores and the ELSA-20 stack show the highest content of C_{org} (chlorins) (Fig. 6).

3.4. Pollen assemblage

The pollen assemblage in this study presented in Fig. 6 is a stack from (i) the two HL cores covering 130,000 to 72,100 yr b2k, (ii) the lower part of core DE3 covering the time span from 72,100 to 59,100 yr b2k (Sirocko et al., 2013, 2016), and (iii) the ELSA-20 stack covering the last 59,100 yr b2k (Sirocko et al., 2022). Three phases of high amount of tree pollen are recorded, which span the intervals of 130,000–118,000 yr b2k (Eemian), 57,000–42,000 yr b2k (early MIS 3), and 10,700 yr b2k to present (Fig. 6). Pollen percentages during the two older periods are dominated by *Pinus* (pine) and *Betula* (birch), as well as *Picea* (spruce) and *Carpinus* (hornbeam) showing increased pollen percentages during these two time periods. Furthermore, *Quercus* (oak) is abundant especially during the Eemian and only very little during early MIS 3 and *Corylus* (hazle) showing higher abundance during the Eemian (Fig. 6, Supplemental Figs. S1, S2, and S3). Typical trees of the temperate mixed forest such as *Quercus* and *Corylus* are most abundant and dominating the forest during the last 10,700 yr b2k interglacial section of the Holocene (Fig. 6). The intervals between the forested periods lack temperate forest species (*Picea*, *Carpinus, Quercus*, *Corylus*) or show only very low percentages of these pollen (118,000–57,000 yr b2k and 42,000–10,700 yr b2k), however, during GIs the forest recovers (Britzius and Sirocko, 2023; Sirocko et al., 2022). Being typical boreal tree species, *Pinus* and *Betula* do not show distinct patterns, probably because both taxa are frost tolerant as well as able to grow on poor soils, resulting in less reaction to changes in climate (San-Miguel-Ayanz et al., 2016). In comparison, Poaceae (grass family) show a distinct pattern and are the dominant plant group whenever temperate forest species decrease during intervals of unfavourable climate (Fig. 6).

3.5. Speleothem growth phases

Compiling all ages from the literature and the new ages from this study (Supplement Table S1) from the four caves (Dechencave,

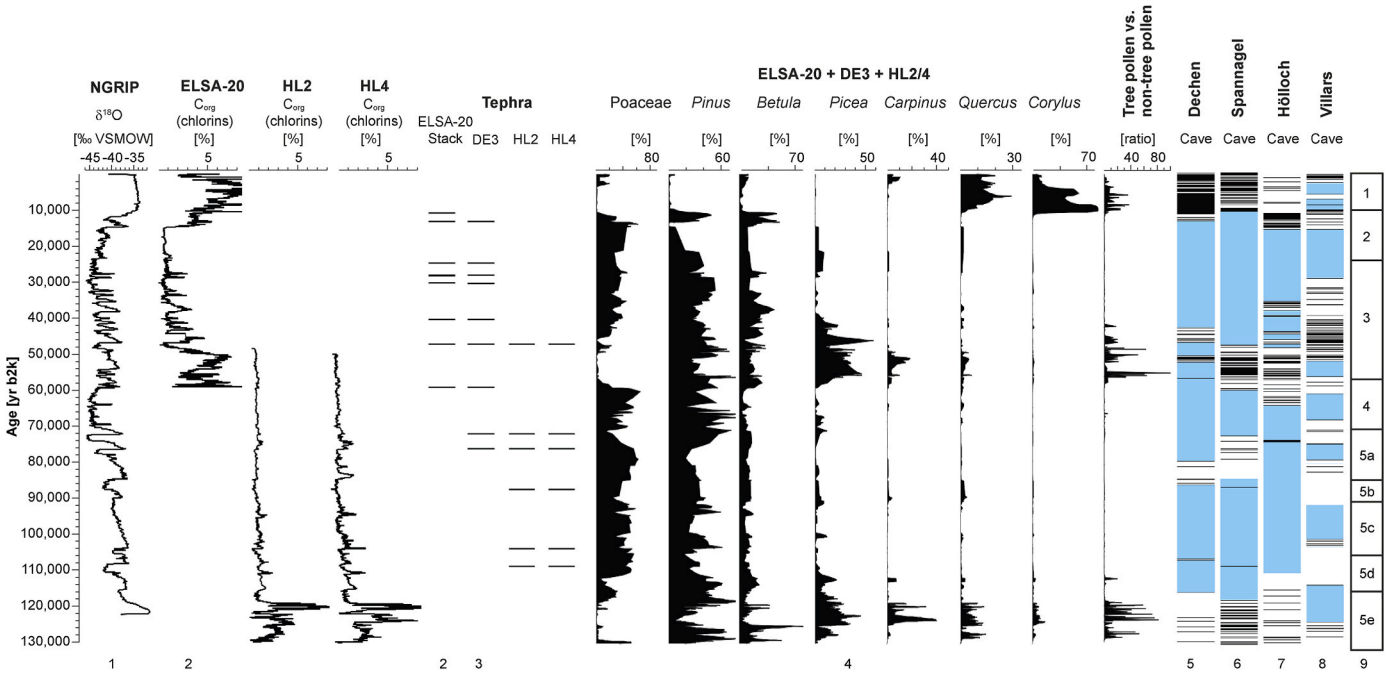

Fig. 6. The $\delta^{18}O$ record of the NGRIP ice core (1) (Rasmussen et al., 2014) is shown for comparison with the C_{org} (chlorins) ELSA-20 stack record (2) (Sirocko et al., 2021) and the C_{org} (chlorins) records from the two cores HL2 and HL4. The marker tephra layers from the ELSA-20 stack (2) (Sirocko et al., 2021) and the core DE3 (3) (Sirocko et al., 2016) are as well indicated as the marker tephra layers in the two cores HL2 and HL4. The different pollen (Poaceae, *Pinus*, *Betula*, *Picea*, *Carpinus*, *Quercus*, *Corylus*) are presented as a stack record from the ELSA-20 stack (4) (Sirocko et al., 2022) combined with the pollen from the lower part of core DE3 (4) (Sirocko et al., 2013, 2016), and the cores HL2 and HL4. Tree vs. non-tree pollen ratio is shown as the last column of the pollen block. Dating from stalagmites and flowstones from four cave systems in central and western Europe are shown in the next four columns. Each horizontal black line represents one $^{230}Th/U$-age. The more ages were determined the denser the lines, forming black areas. Light blue areas represent times with no speleothem growth in the corresponding caves resulting from the calculated age models of the different speleothems. White areas represent times of speleothem growth calculated in the age models of the speleothems in the underlying studies. Stalagmite datings are from Bunker Cave, B7-Cave, Hüttenbläserschacht Cave, and Dechencave from western Germany (5) (Fohlmeister et al., 2012; Niggemann et al., 2003; Riechelmann et al., 2023; Waltgenbach et al., 2020, 2021; Weber et al., 2018, 2021). Stalagmites from the Austrian Alps are from Spannagel and Kleegruben Cave (6) (Fohlmeister et al., 2013; Holzkämper et al., 2004, 2005; Moseley et al., 2014; Spötl et al., 2006a, 2007, 2008; Spötl and Mangini, 2007). Dated stalagmites from the German/Austrian Alps are from Hölloch Cave (7) (Li et al., 2021; Moseley et al., 2014, 2015, 2020; Wurth et al., 2004). Villars Cave in western France is the fourth cave with dated stalagmites in this compilation (8) (Genty et al., 2002, 2003, 2006, 2010; Labuhn et al., 2015; Wainer et al., 2009, 2011). The division of the Marine Isotope Stages (MIS) is given after (9) Lisiecki and Raymo (2005).

Hüttenbläserschacht Cave, B7-Cave, Bunker Cave) in western Germany (Fohlmeister et al., 2012; Niggemann et al., 2003; Riechelmann et al., 2023; Waltgenbach et al., 2020, 2021; Weber et al., 2018, 2021), it results in pronounced stalagmite growth phases during the Eemian and during MIS 5a. Two prominent growth phases are detected during early MIS 3 as well as stalagmite growth during the last 13,600 yr b2k (Fig. 6, Supplemental Table S1). Stalagmite growth in the Austrian Alps (Spannagel and Kleegruben Cave) show a relatively similar pattern to the caves in western Germany, with stalagmite growth during the Eemian, a longer growth phase during MIS 5a, during early MIS 3, and during the last 10,800 yr b2k (Fohlmeister et al., 2013; Holzkämper et al., 2004, 2005; Moseley et al., 2014; Spötl et al., 2006a, 2007, 2008; Spötl and Mangini, 2007) (Fig. 6). The stalagmites from the Hölloch Cave in the German/Austrian Alps grew during the Eemian, a pronounced growth phase starting in MIS 4 and several growth phases during the MIS 3, and speleothem growth is detected throughout the entire last 15,700 yr b2k (Li et al., 2021; Moseley et al., 2014, 2015, 2020; Wurth et al., 2004) (Fig. 6). The fourth cave in this compilation is Villars Cave in western France where speleothem growth is detected during the early Eemian, MIS 5d to 5c, and MIS 5b to 5a. Further growth phases are also detected during parts of MIS 4 and a long phase of speleothem growth is detected during MIS 3, as well as four growth phases during the last 15,300 yr b2k (Genty et al., 1999, 2002, 2003, 2006, 2010; Labuhn et al., 2015; Wainer et al., 2009, 2011) (Fig. 6).

For all ages the dating uncertainties have to be taken into account. They vary from ±10–4000 years for the caves in western Germany, ±4–2800 years for Spannagel Cave, ±37–5564 years for Hölloch Cave, and ±27–9477 years for Villars Cave. This is a quite wide and relatively similar range for all four caves. The dating uncertainties are influenced by the time when the analyses were performed due to the improvement in mass spectrometry sensitivity during the last decades (Cheng et al., 2013; Scholz and Hoffmann, 2008) as well as by their detrital content, which results in higher uncertainties due to the correction (Ludwig, 2003).

4. Discussion

4.1. Proxy record interpretation

4.1.1. Bioproductivity in the Eifel

The combination of the high resolution (six months on average) C_{org} (chlorins) record of the ELSA-20 stack (Sirocko et al., 2021) with the C_{org} (chlorins) records of the two HL cores from this study, which have an average resolution of three years (HL2) and two years (HL4), respectively, shows three phases of high C_{org} (chlorins) content. These phases are during the Eemian, the early MIS 3, and the last 14,000 yr b2k (Fig. 6), indicating warm climate conditions in the Eifel region. The C_{org} (chlorins) content, mainly arising from chlorophyll of diatoms and chrysophytes, is a proxy for the bioproductivity in the lake, which is sensitive to temperature changes and nutrient supply. Therefore, C_{org} (chlorins) content can be used to reconstruct past temperature variabilities as presented in the study of Sirocko et al. (2021) for the last 59, 100 yr b2k, indicating that the millennial scale temperature variability in the Eifel region is related to temperature changes in the North Atlantic

Ocean and Greenland. Therefore, due to the very high resolution of these proxy records, it is possible to detect the GIs (Fig. 5) as they are named in the NGRIP $\delta^{18}O$ record (North Greenland Ice Core Project, 2004; Rasmussen et al., 2014) or also named D/O-events (Dansgaard et al., 1993). This enables the tuning of the C_{org} (chlorins) records to the NGRIP $\delta^{18}O$ record (Rasmussen et al., 2014), in the framework of the anchor dating by the marker tephra layers (see sections 3.2 and 3.3, Fig. 5, and Table 2). The dating uncertainties of the NGRIP $\delta^{18}O$ record are transferred by the tuning to the C_{org} (chlorins) records (Fig. S4) and therefore, highly improved the dating uncertainties of the $^{40}Ar/^{39}Ar$-dating of the tephra layers. The NGRIP $\delta^{18}O$ record has an increasing dating uncertainty with depth up to 2573 years of maximum layer counting error at 59,440 yr b2k and not available errors for the deeper part of the ice core up to 119,140 yr b2k (Rasmussen et al., 2014). Errors for the older part are estimated as $\geq$ 2573 years.

A critical point of the HL sediment cores is the change in the sedimentation process in the lake from annual varves to an event lamination around 90,000 yr b2k ago (Fig. 4b). This may have an influence on the preservation of the C_{org} (chlorins) in the sediment due to no thermal stratification during the event lamination sedimentation (Fig. 4a and b). However, around 90,000 yr b2k no distinct changes in the two C_{org} (chlorins) records are detected (Fig. 5b and c). Therefore, it can be assumed that the preservation of the C_{org} (chlorins) was not affected to a larger extent. To conclude, C_{org} (chlorins) is a temperature proxy in particular sensitive to short term temperature changes related to GIs (D/O-events), which only last for centuries to millennia (Rasmussen et al., 2014).

4.1.2. Vegetation changes in the Eifel

The forest in the Eifel during the Eemian had an abundance of temperate forest species, such as *Quercus*, *Corylus,* and *Carpinus* as well as *Picea* (Sirocko et al., 2005) (Fig. 6). A developed forest vegetation during MIS 5c and 5a is not detected in the pollen record from the Eifel region (Fig. 6), indicating that MIS 5c and 5a were colder than early MIS 3 in the Eifel region. The forest during the early MIS 3 (57,000 to 42,000 yr b2k) was dominated by *Picea* and *Carpinus* (Sirocko et al., 2013, 2016, 2022), species such as *Quercus* and *Corylus* were not or only very little abundant (Fig. 6). This indicates warm climate during early MIS 3, even if it was colder than during the Eemian and the last 10,700 yr b2k (Sirocko et al., 2016). The abundance of *Quercus* and *Corylus* was very high during the last 10,700 yr b2k (Sirocko et al., 2016), which indicates a mean annual temperature higher than 5 °C (San-Miguel-Ayanz et al., 2016). However, the pollen assemblage during the last 6300 yr b2k is influenced by anthropogenic activities (e.g., Litt et al., 2009). Furthermore, *Pinus* and *Betula* show relatively constant abundance during the complete last glacial cycle except the last 10,700 yr b2k and *Pinus* during parts of the Eemian. During the times between the three forested periods (MIS 5d to 5a, MIS 4, late MIS 3, and MIS 2) the vegetation is dominated by Poaceae, as well as *Pinus* in the Eifel region (Sirocko et al., 2022) indicating colder climate conditions and the loss of dense forest. The pollen record is as well sensitive to shorter temperature changes in relation to the GIs (Britzius and Sirocko, 2023; Sirocko et al., 2022), however, this is not the focus of this study.

Comparing this pollen record with other pollen records from central and western Europe, using the tree pollen vs. non-tree pollen ratio for all records, the picture is not consistent (Fig. 7). The pollen record from Füramoos in southern Germany shows forest during the Eemian and some increase in tree pollen during MIS 5d decreasing into 5c as well as during the last 14,000 yr b2k. During MIS 3, a tundra vegetation is detected. This record is quite continuous only showing a hiatus from

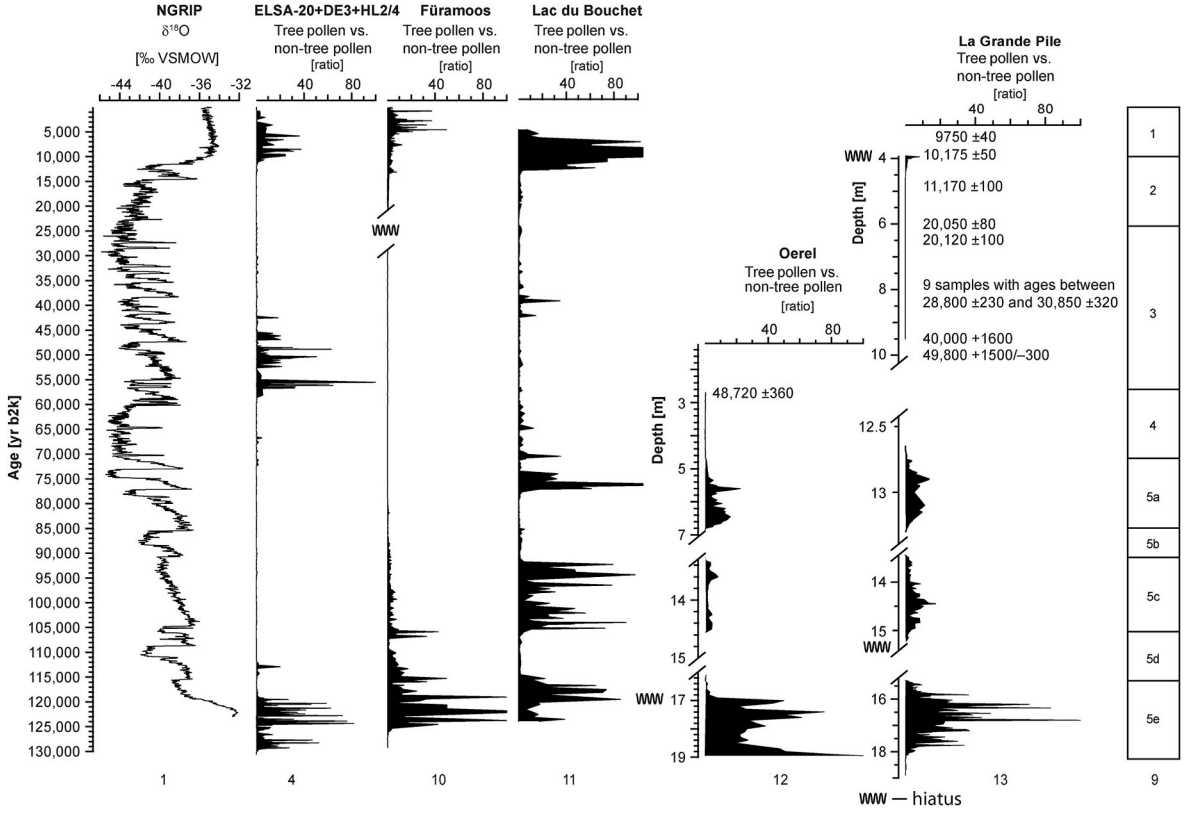

Fig. 7. The NGRIP $\delta^{18}O$ record (1) (Rasmussen et al., 2014) is shown for comparisons with the tree pollen vs. non-tree pollen ratio records of the Eifel stack record (ELSA-20 + DE3 + HL2/4) (4) (Sirocko et al., 2013, 2016, 2022), Füramoos in southern Germany (10) (Kern, 2021), Lac du Bouchet in the Massif Central (France) (11) (de Beaulieu and Reille, 2018), Oerel in northern Germany (12) (Behre et al., 2005; Behre and van der Plicht, 1992), and La Grande Pile in the Vosges Mountains (France) (13) (de Beaulieu and Reille, 1992; Woillard and Mook, 1982). For the two records Oerel and La Grande Pile no age depth models are available. Ages of the ^{14}C-datings are displayed for these two records. The division of the Marine Isotope Stages (MIS) shown on the right site is given after (9) Lisiecki and Raymo (2005).

28,000 to 20,000 yr b2k (Fig. 7) (Kern et al., 2022). Another long and continuous pollen record is from Lac du Bouchet in the Massif Central (France), which shows four phases with pronounced forest during MIS 5e, 5c, and 5a as well as during the last 14,000 yr b2k. Furthermore, a little increase in tree pollen is detected around 40,000 yr b2k during MIS 3 (Fig. 7). MIS 3 is dominated by *Pinus* and steppe vegetation at this site (de Beaulieu et al., 2001), which is also detected in the Eifel during late MIS 3 (Fig. 6). The three forested phases during MIS 5e, 5c, and 5a are also detected in a review of central and northern European pollen records, from the sites Oerel in northern Germany and La Grande Pile in the Vosges Mountains (France) (Fig. 7) (Helmens, 2014), which are the sites from this review nearest to the Eifel. In comparison to the Lac du Bouchet record, where MIS 5e, 5c, and 5a show similar amounts of tree pollen, the pollen records from Oerel and La Grande Pile show the strongest forest abundances during MIS 5e, while during MIS 5c and 5a less tree pollen are detected (Helmens, 2014). Furthermore, the record from Oerel is interrupted by sand deposits without pollen during the cold phases (MIS 5d and 5b) and shows a hiatus after MIS 5e. In addition, the chronology is based on ^{14}C-dating in the period up to 50,000 yr b2k (Fig. 7). For MIS 3, a shrub tundra is detected from the Oerel record (Helmens, 2014). The pollen record of La Grande Pile has a hiatus in the MIS 5d and the chronology is based on ^{14}C-datings up to 50,000 yr b2k. The older section was not independently dated (Fig. 7). For MIS 3, an open *Betula-Pinus* forest is detected at this site (Helmens, 2014), which is comparable to the Eifel region (Fig. 6). In addition, the review of Fletcher et al. (2010) also interpreted an open boreal forest in central and western Europe during multiple intervals (D/O-events) of relatively warm and humid climate during MIS 3.

In summary, these records from central and western Europe do not show a consistent pattern, even if divided into subregions. The three forested phases during MIS 5 are detected in France and northern Germany and also the two French sites differ in the magnitude of forest during MIS 5e, 5c, and 5a. However, a pronounced forested phase during the early MIS 3 is only detected from the Eifel and - to a little extent - in Lac du Bouchet (Fig. 7), even though the same species are also detected at the other sites. Therefore, the pollen results from the Eifel are at the first sight surprising in comparison to the pollen records of the other lakes and peat bogs in central and western Europe (de Beaulieu et al., 2001; Helmens, 2014; Kern et al., 2022). One potential explanation for the differences may be the only partial age control of most of the European Eemian and last glacial cycle pollen records (Felde et al., 2020; Helmens, 2014). In the time period up to the limit of radiocarbon dating of 55,000 yr b2k (Hajdas et al., 2021), the age control of pollen sequences is better (Fletcher et al., 2010). Some European records are also dated by OSL beyond the ^{14}C-dating range (Engels et al., 2008a; Helmens and Engels, 2010) but unfortunately not the records from central and western Europe used here for comparison. However, hiatuses detected in the older parts of the records from Oerel and La Grande Pile are not dated and, therefore, their exact timing and duration are unknown bearing the potential that the increase in tree pollen in these records after the hiatuses could be related to a younger age or the phase with a high amount of tree pollen before the hiatuses to an older age. In this case, the proxy records from the Eifel maar lake sediments have the advantage of the tephra layers, which are partly absolutely dated and give anchor points for the chronology and furthermore, that the C_{org} (chlorins) record is such a sensitive temperature proxy allowing the tuning to the NGRIP δ^{18}O record, which highly improves the age control of the proxy records from the Eifel.

4.1.3. Speleothem growth

Pronounced speleothem growth occurs in western Germany (including: Dechencave, Hüttenbläserschacht Cave, B7-Cave, Bunker Cave) during the warm and humid phases, such as during the Eemian and MIS 5a, the two warmest and humid phases during early MIS 3 (Weber et al., 2018), and the last 13,600 yr b2k (Fohlmeister et al., 2012; Riechelmann et al., 2023; Waltgenbach et al., 2020, 2021; Weber et al., 2021). This region was under the influence of permafrost at least during the last glacial (MIS 2), which is proven by the occurrence of cryogenic cave calcites in the Dechencave (Richter et al., 2018) and Hüttenbläserschacht Cave (Richter et al., 2015). Therefore, the compilation of the dating of the different speleothems from these caves indicate growth during interglacial periods and no speleothem growth during glacial periods or cold and dry period with less soil and/or vegetation.

The growth of speleothems in the high alpine Spannagel Cave (including Kleegruben Cave) on an elevation of 2500 m asl is very sensitive to glacial periods in which no stalagmite growth occurs (Holzkämper et al., 2005; Spötl and Mangini, 2007). The region of these two caves is only ice free during the warmest periods of the interglacial periods of the Eemian and the Holocene reconstructed from the sediment deposits of the glacier (Fohlmeister et al., 2013; Spötl and Mangini, 2007). During the times in between the caves were covered by the Hintertux Glacier. However, only during glacial times the glacier does not have water at its base and the cave temperature falls below freezing and no speleothem growth was possible (Spötl et al., 2007). During the other periods the glacier was a temperate glacier with melt water at its base and a cave temperature slightly above freezing (Spötl et al., 2006a). Furthermore, the gneiss and marble host rock of Spannagel Cave includes pyrite which is oxidised by the seeping water and produces sulfuric acid, which dissolves the marble, producing excess CO_2 and therefore, supersaturated drip water and speleothem formation is possible without vegetation and soil above the cave (Holzkämper et al., 2004; Spötl and Mangini, 2007). This makes the speleothem growth phases of the Spannagel Cave very sensitive to the coldest glacial periods. The periods with no growth in Spannagel Cave correspond quite well to the phases of no speleothem growth in the caves in western Germany not only including MIS 4, late MIS 3, and MIS 2 but also MIS 5d to 5b (Fig. 6).

Hölloch Cave is located at 1440 m asl in the Alps with a today thin and patchy soil cover and vegetation, which is dominated by grass, shrubs, and scattered trees (Wurth et al., 2004). Due to similarities of the proxy records from Hölloch Cave stalagmites with the NGRIP δ^{18}O record, a common North Atlantic climate forcing is assumed (Li et al., 2021; Moseley et al., 2020). The alpine region of Hölloch Cave was below glaciers at least during the maximum of the MIS 2 (Geologische Bundesanstalt von Österreich, 2013). However, during times the cave was covered with glaciers and also during permafrost conditions, no speleothem growth was possible, as well as during cold periods with no soil and vegetation (cf., Moseley et al., 2015), also, when the glacier above this cave was a temperate one with water at its base. The host rock is limestone and does not have this speciality as the host rock of Spannagel Cave with the high amount of pyrite. In comparison to the speleothem growth phases in western Germany and in Spannagel Cave, the speleothem growth patterns in Hölloch Cave are relatively similar (Fig. 6).

Speleothem growth in Villars Cave stopped during cold periods such as MIS 4 and MIS 2 (Fig. 6) due to the formation of permafrost above the cave (Genty et al., 2003, 2010; Wainer et al., 2009). Further growth stops, which are not related to cold phases can also be induced by flooding of the cave (Genty et al., 2003) or too dry conditions as assumed during the Younger Dryas (Genty et al., 2006). Due to the location of the cave near to the Atlantic an influence of North Atlantic circulation changes is most likely (Genty et al., 2010). In comparison to the other three cave systems the periods of no speleothem growth during glacial times and colder periods are shorter in Villars Cave. This is most probably due to its more southern location with an on average warmer climate, which results in shorter periods of permafrost in the past. Therefore, growth stops during MIS 5e, 5c, and 5a can also be related to other reasons in this cave as described above.

One study from Villars Cave interpreted continuous speleothem growth over the last 50,000 yr b2k (Wainer et al., 2011), which contradicts three other studies from this cave indicating that speleothem

growth stopped at 29,000 yr b2k (Genty et al., 2003, 2010; Wainer et al., 2009). The age model of this first mentioned study interprets continuous growth between 30,000 yr b2k until present with only two ages, one around 32,000 yr b2k and one at 10,000 yr b2k (Wainer et al., 2011), which we do not consider as a valid age model. Wainer et al. (2011) mention a discontinuity between these two ages, which is most probably an indication for discontinuous growth. Therefore, assuming a stop of speleothem growth at 30,000 yr b2k, is much more realistic also in comparison to the other studies from Villars Cave, considering the start of the MIS 2 glacial period.

We note that the published ages of all stalagmites and the dating density (more black lines in Figs. 6 and 8) may be biased by the underlying goals of the specific projects and studies, which had been for example a focus on the Eemian (Holzkämper et al., 2004; Moseley et al., 2015; Spötl et al., 2002), the MIS 3 with its D/O-events (Genty et al., 2003, 2010; Moseley et al., 2014; Spötl et al., 2006b; Weber et al., 2018), or the Holocene (Fohlmeister et al., 2012, 2013; Riechelmann et al., 2023). Furthermore, the dating density also depends on when the studies were conducted because the analyses got less time consuming and sample amount decreased during the last decades enabling the analysis of more ages (Cheng et al., 2013; Scholz and Hoffmann, 2008). However, all four cave systems show similarities in their time periods of no speleothem growth during the glacial periods of MIS 4 and 2, as well as during MIS 5d to 5b (except Villars Cave) (Fig. 6), which indicate a supra-regional climate forcing.

4.2. Comparing the proxy records during the last 130,000 yr b2k

The comparison of all proxy records reveals that speleothems grew mainly during phases of temperate forest vegetation and thus soil development, as well as phases of high bioproductivity in the Eifel (Fig. 8). However, speleothems from Dechencave and Spannagel Cave also show pronounced growths during MIS 5a (Fig. 6), which do not show a corresponding warm phase in the Eifel. This indicates especially for Spannagel Cave climate conditions, which were warm enough that the glacier above the cave got temperate and liquid water was available. The absence of speleothem growth in Spannagel Cave during MIS 5c is explained by a strong glacial advance during MIS 5d, corresponding to a pronounced drop in sea level by 60 m from the Eemian (Fig. 8), and the following warming during MIS 5c was interpreted as insufficient in length or overall colder, which inhibit speleothem growth (Holzkämper et al., 2005). The speleothem growth phases in Villars Cave are longer and also show speleothem growth during MIS 5d, 5b, and 5a (Fig. 6), which is not completely consistent with the French pollen records from Lac du Bouchet (de Beaulieu et al., 2001) and La Grande Pile (de Beaulieu and Reille, 1992) (Fig. 7). However, these results indicate

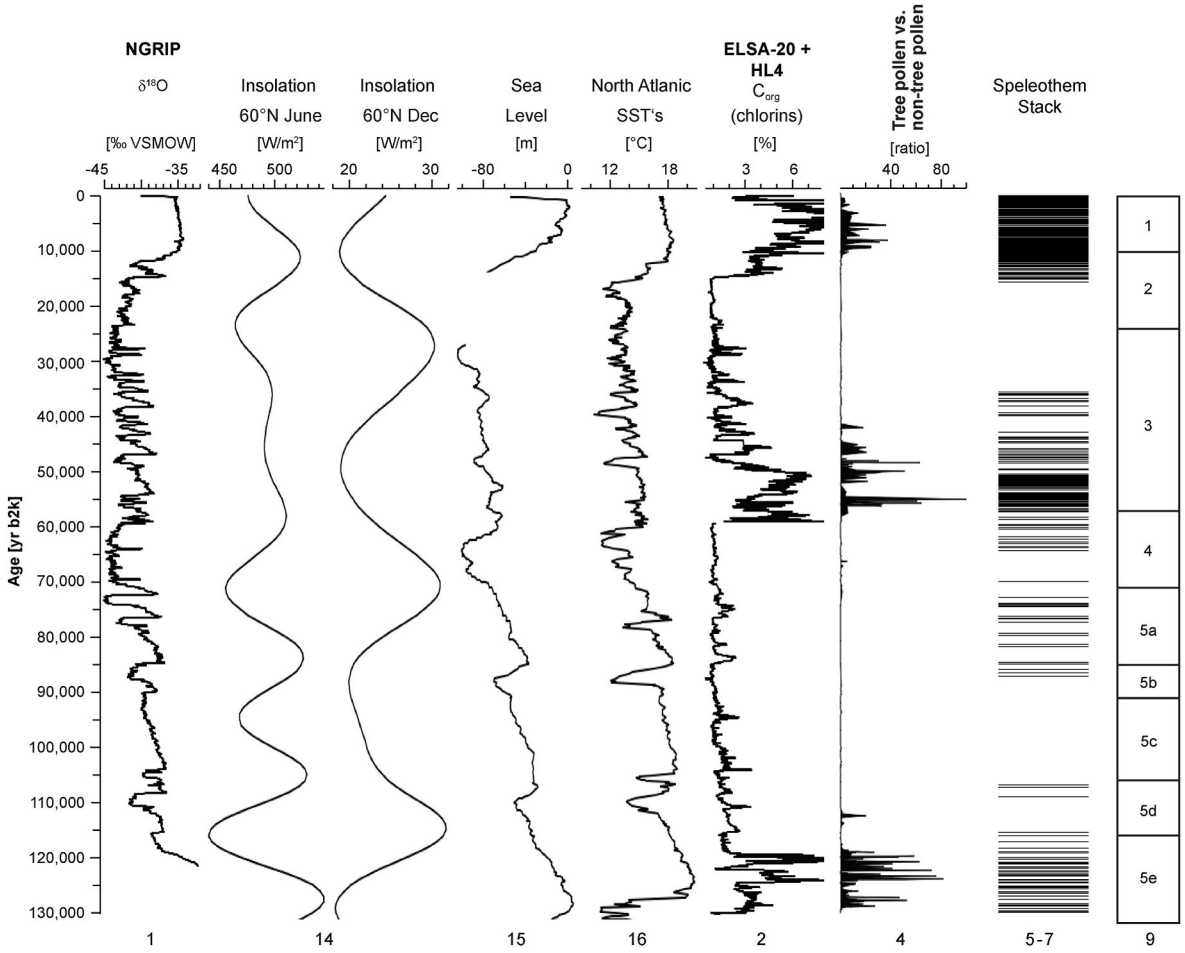

Fig. 8. The NGRIP $\delta^{18}O$ record (1) (Rasmussen et al., 2014), the June and December insolation at 60°N (14) (Berger and Loutre, 1991), sea level (15) (Grant et al., 2014), and North Atlantic sea surface temperatures (SST's) (16) (Martrat et al., 2007) are shown for comparison with the C_{org} (chlorins) ELSA-20 stack (2) (Sirocko et al., 2021) and core HL4. The stack record of tree vs. non-tree pollen ratio (4) (Sirocko et al., 2013, 2016, 2022) and the stack of datings from speleothems from the three cave systems in central Europe (Dechencave, Spannagel Cave, Hölloch Cave) are shown. The black lines indicate $^{230}Th/U$-ages (see figure cation of Fig. 6); (5) (Fohlmeister et al., 2012; Niggemann et al., 2003; Riechelmann et al., 2023; Waltgenbach et al., 2020, 2021; Weber et al., 2018, 2021), (6) (Fohlmeister et al., 2013; Holzkämper et al., 2004, 2005; Moseley et al., 2014; Spötl et al., 2006a, 2007, 2008; Spötl and Mangini, 2007), (7) (Li et al., 2021; Moseley et al., 2014, 2015, 2020; Wurth et al., 2004). The division of the Marine Isotope Stages (MIS) is given after (9) Lisiecki and Raymo (2005).

warmer climate conditions and shorter durations of the glacial or cold periods in France than in the Alps and Germany.

Early MIS 3 is pronounced in the pollen and C_{org} (chlorins) records from the Eifel as well as in the speleothem growth especially from the two Alpine sites (Spannagel Cave and Hölloch Cave) and western Germany indicating warm and wet climate during this period, warmer than during at least MIS 5c. Warmer climate during MIS 5c and 5a would be expected due to the high summer insolation (Berger and Loutre, 1991) during the beginning of MIS 5c and 5a (Fig. 8). Further comparison of these proxy records to hemispherical records such as the North Atlantic sea surface temperature (Martrat et al., 2007), sea level (Grant et al., 2014), and the NGRIP $\delta^{18}O$ record (Rasmussen et al., 2014), the MIS 3 is not as pronounced in these records as MIS 5c and 5a, which do have higher SSTs by on average 3 °C and higher sea level by on average 20 m than the MIS 3 (Fig. 8). The $\delta^{18}O$ in the NGRIP record is approximately on a similar maximum level during MIS 3 and MIS 5c but MIS 5c has higher minimum values than MIS 3. Furthermore, the GIs corresponding to MIS 5c and 5a are longer than the ones during MIS 3 (Fig. 8). Comparison of the 60°N June insolation (Berger and Loutre, 1991) with the NGRIP $\delta^{18}O$ record, sea level, and SST's indicates that the summer insolation is a major driver of the climate variability shown by these records representing the North Atlantic climate (Fig. 8). All these detected warm periods are related to summer insolation maxima. However, the proxy records from the Eifel show a partially decoupling from the North Atlantic on this long-term orbital scale variability during the time between the end of the Eemian and the last 14,000 yr b2k by showing a warmer early MIS 3 than MIS 5c and 5a (Fig. 8). Therefore, additional climate forcings and/or triggers must play a role for climate variability in central and western Europe potentially resulting in different local climate conditions as indicated by the differences in the central and western European pollen records (Fig. 7).

The site of Füramoos is located in the alpine foreland and therefore near to the Alpine ice sheet (Ehlers et al., 2011), which could result in quite cold climate conditions not favorable for forest vegetation at this location between the warmest interglacial times of the Eemian and the Holocene. Due to its southern and therefore on average warmer location in the Massif Central (France), the record from Lac du Bouchet probably indicates the warmest climate conditions of the presented sites with the quite pronounced forest vegetation during MIS 5e, 5c, and 5a as well as a short phase of forest vegetation during MIS 3. However, a warmer climate with pronounced forest vegetation during MIS 5c and 5a would also expect a pronounced forest during MIS 3, which is not detected. It is possible that the climate was too dry at this site for a pronounced forest during MIS 3 although there is pronounced speleothem growth in Villars Caves in western France during MIS 3 indicating warm and wet climate conditions (Fig. 6). Probably the atmospheric circulation was different during MIS 3 in comparison to the Eemian and the Holocene related to the Alpine and Fennoscandian ice sheets. If this contrasting pattern, between the pollen record and speleothem growth, is related to precipitation, it can be due to a luv situation at Villar Cave and a lee situation at Lac du Bouchet with the Massif Central in between when winds were predominant from the west during MIS 3.

The site of the pollen record from La Grande Pile is located north-east of Lac du Bouchet and also a bit nearer to the Alps with its ice sheet during glacial times (Ehlers et al., 2011). However, these colder conditions could be a reason for the lower amount of tree pollen during MIS 5c and 5a. The same pattern is detected in the pollen record of Oerel, which is the most northern site in this compilation, which could be a reason for not showing a forest vegetation during MIS 3 due to the proximity to the Fennoscandian ice sheet. The detected forest vegetation during MIS 5c and 5a in Oerel could be due to a farer distance to the Fennoscandian ice sheet and therefore warmer conditions at this site. However, as discussed above, the problem of precise dating of these records beyond the ^{14}C-dating range could also be a possible reason for these discrepancies (see section 4.1.2).

Furthermore, a review of European pollen records interpreted that the climate variability during the last glacial cycle was mostly related to the degree of continentality, which increased after the MIS 5e. This change to more continentality during MIS 5c and 5a results in changes to lower winter temperature, which are related to lower winter insolation (Fig. 8), less precipitation, and constant summer temperatures, which results in a shorter growing season (Helmens, 2014). Lower winter temperatures have an inhabiting influence on temperate forest species such as *Quercus* and *Corylus* (Salonen et al., 2012). This could be a potential explanation for no forest during MIS 5c and 5a in the pollen record and probably also no pronounced C_{org} (chlorins) content in these time periods from the Eifel.

A hypothesis for the MIS 3 is that the mean temperatures are lower than during MIS 5c and 5a, indicated by SST's and sea level (Fig. 8), however, the seasonality is weaker (less continental climate with lower summer temperatures and higher winter temperatures), which favors tree species, such as *Picea* and *Carpinus* (Fig. 6). The forcing of this may be the insolation because of relatively high summer insolation and also winter insolation is not at the minimum and still decreasing during early MIS 3 (Fig. 8). Furthermore, pollen and chironomids records from northern Finland indicate summer temperatures similar to present day during early MIS 3 (Helmens and Engels, 2010). Furthermore, four forested phases are detected from northern Finland during MIS 5e, 5c, 5a, and MIS 3 indicating warm temperatures during all these phases (Helmens, 2014). However, also other forcings such as seasonal atmospheric circulation changes, vegetation, and/or the Fennoscandian ice sheet can play a role and influence the local climate conditions.

Overall, this topic needs further research with more well dated pollen sequences covering the entire last glacial cycle as well as comparing the pollen records to other climate proxy records. However, this is a challenging task due to problems of dating pollen records beyond the ^{14}C-dating range and not so often used OSL dating. Precise dating of speleothem growth phase during this time period should be improved. Furthermore, there are a lot of caves in central and western Europe bearing the potential to find and date new speleothems growing during the last glacial cycle.

5. Conclusions

The stacked pollen record indicates three forested phases in the Eifel. During the Eemian (MIS 5e) and the last 10,700 yr b2k the forest is dominated by temperate tree species (*Quercus* and *Corylus*) and during the early MIS 3 by *Picea* and *Carpinus*, which were also abundant during the Eemian. Between the forested periods the vegetation is dominated by Poaceae indicating colder climate. These three forested phases correspond to high C_{org} (chlorins) content and are also corresponding to speleothem growth phases in western Germany and the Alps. The speleothem growth in these caves is sensitive to glacial, permafrost, as well as cold and dry climate conditions. However, Villars Cave in western France shows longer speleothem growth periods as the three other cave systems probably related to warmer climate. Pollen records from France and northern Germany showing three forested phases during the MIS 5e, 5c, and 5a, indicating warm climate. The pollen records from the Eifel and southern Germany do not show the expected three forested phases during the MIS 5. The speleothems from western Germany and the Alps show growth during MIS 5a indicating as well warmer climate. However, the picture is not consistent. A European pollen review interpreted that the climate got more continental after the Eemian, with lower winter temperatures and summer temperatures staying on the same level. This should have an influence on the growing season and therefore, on the vegetation and temperate forest species are not favoured. This is a possible explanation of the missing of the two further forested phases in the Eifel. The forested phase detected in the pollen record from the Eifel during early MIS 3, which corresponds quite well to speleothem growth phases in western Germany, the Alps, and western France, is probably related to a phase with less continental climate conditions with lower summer temperatures and higher winter temperatures induced by

the insolation.

However, further research of pollen, C_{org} (chlorins) from lake sediments and peat bogs, as well as speleothem growth phases from the entire last glacial cycle from central and western Europe are necessary for a better understanding of the supra-regional climate variability and its forcings.

Authors contributions

D.F.C.R, Conceptualisation, Methodology, Validation, Formal analysis, Investigation, Resources, Writing original draft, Visualisation, Funding acquisition, J.A, Validation, Formal analysis, Investigation, Writing original draft, Writing review & editing, Visualisation, S.B, Validation, Formal analysis, Investigation, Writing original draft, Writing review & editing, Visualisation, F.K, Validation, Formal analysis, Investigation, Writing review & editing, Visualisation, D.S, Resources, Writing review & editing, Funding acquisition, F.S, Conceptualisation, Methodology, Validation, Writing original draft, Writing review & editing, Supervision, Project administration, Funding acquisition, K.P.J, Validation, Investigation, Resources, Visualisation, F. Sch: Validation, Formal analysis, Investigation, Resources, Writing original draft, Writing review & editing, Visualisation.

Data availability

Data are available on the Pangaea database and on the web site of the ELSA-project https://elsa-project.de.

Declaration of competing interest

The authors declare that they have no known competing financial interests or personal relationships that could have appeared to influence the work reported in this paper.

Acknowledgments

D. F. C. Riechelmann, D. Scholz, and F. Sirocko are grateful to the PalMod Project funded by the BMBF (Bundesministerium für Bildung und Forschung) and the DLR (Deutsche Gesellschaft für Luft-und Raumfahrt) as well as to the DFG (Deutsche Forschungsgemeinschaft) (FKZ: 01LP1510B; SCHO 1274/13–1; SCHO 1274/13–2; RI 2136/2-2; INST247/889-1 FUGG) for funding. We thank the Team from the Dechencave and German Cave Museum as well as the Speleogroup Letmathe e.V. for the permission and help during sampling of stalagmites from the Dechencave. For the help during the measurements with the Nu plasma we have to thank B. Stoll and U. Weis at the Max Planck Institute for Chemistry Mainz. For help during preparation and dating of speleothem sample with the Thermo Scientific Neptune Plus we have to thank M. Groβkopf and R. Mertz-Kraus. Furthermore, we thank the Stölben Drilling Company (Cochem, Germany) for drilling the sediment cores. F. Dreher is thanked for sample preparation and counting of the pollen, K. Schwibus for technical support and sample preparation, M. Engel for the C_{org}(chlorins) measurements, F. Fuhrmann for data processing, and P. Sigl for graphical editing. We thank three anonymous reviewers for their constructive comments, which highly improved the manuscript and J. Xiao for his editorial work.

Appendix A. Supplementary data

Supplementary data to this article can be found online at https://doi.org/10.1016/j.quaint.2023.11.001.

References

Ampel, L., Wohlfarth, B., Risberg, J., Veres, D., Leng, M.J., Tillman, P.K., 2010. Diatom assemblage dynamics during abrupt climate change: the response of lacustrine diatoms to Dansgaard–Oeschger cycles during the last glacial period. J. Paleolimnol. 44, 397–404.

Behre, K.-E., Hölzer, A., Lemdahl, G., 2005. Botanical macro-remains and insects from the Eemian and Weichselian site of Oerel (northwest Germany) and their evidence for the history of climate. Veg. Hist. Archaeobotany 14, 31–53.

Behre, K.-E., van der Plicht, J., 1992. Towards an absolute chronology for the last glacial period in Europe: radiocarbon dates from Oerel, northern Germany. Veg. Hist. Archaeobotany 1, 111–117.

Berger, A., Loutre, M.F., 1991. Insolation values for the climate of the last 10 million years. Quat. Sci. Rev. 10, 297–317.

Berglund, B.E., Ralska-Jasiewiczowa, M., 1986. Pollen analysis and pollen diagrams. In: Berglund, B.E. (Ed.), Handbook of Holocene Palaeoecology and Palaeohydrology. John Wiley & Sons, Chichester, pp. 455–486.

Böhm, E., Lippold, J., Gutjahr, M., Frank, M., Blaser, P., Antz, B., Fohlmeister, J., Frank, N., Andersen, M.B., Deininger, M., 2015. Strong and deep Atlantic meridional overturning circulation during the last glacial cycle. Nature 517, 73–76.

Bolland, A., Kern, O.A., Koutsodendris, A., Pross, J., Heiri, O., 2022. Chironomid-inferred summer temperature development during the late Rissian glacial, Eemian interglacial and earliest Würmian glacial at Füramoos, southern Germany. Boreas 51, 496–516.

Britzius, S., Sirocko, F., 2023. Vegetation dynamics and megaherbivore presence of MIS 3 stadials and interstadials 10–8 obtained from a sediment core from Auel infilled maar, Eifel, Germany. Quaternary 6, 44.

Cheng, H., Lawrence Edwards, R., Shen, C.-C., Polyak, V.J., Asmerom, Y., Woodhead, J., Hellstrom, J., Wang, Y., Kong, X., Spötl, C., Wang, X., Calvin Alexander Jr., E., 2013. Improvements in 230Th dating, 230Th and 234U half-life values, and U–Th isotopic measurements by multi-collector inductively coupled plasma mass spectrometry. Earth Planet Sci. Lett. 371–372, 82–91.

Dansgaard, W., Johnsen, S.J., Clausen, H.B., Dahl-Jensen, D., Gundestrup, N.S., Hammer, C.U., Hvidberg, C.S., Steffensen, J.P., Sveinbjörnsdottir, A.E., Jouzel, J., Bond, G., 1993. Evidence for general instability of past climate from a 250-kyr ice-core record. Nature 364, 218–220.

de Beaulieu, J.-L., Andrieu-Ponel, V., Reille, M., Grüger, E., Tzedakis, C., Svobodova, H., 2001. An attempt at correlation between the Velay pollen sequence and the Middle Pleistocene stratigraphy from central Europe. Quat. Sci. Rev. 20, 1593–1602.

de Beaulieu, J.-L., Reille, M., 2018. Pollen Profile LIMAGNE3, Limagne, France. PANGAEA.

de Beaulieu, J.L., Reille, M., 1992. The last climatic cycle at La Grande Pile (Vosges, France) a new pollen profile. Quat. Sci. Rev. 11, 431–438.

Degering, D., Krbetschek, M.R., 2007. Dating of interglacial deposits by luminescence methods. In: Sirocko, F.e.a. (Ed.), The Climate of Past Interglacials. Elsevier, pp. 157–172.

Ehlers, J., Gibbard, P.L., Hughes, P.D., 2011. Quaternary Glaciations - Extent and Chronology. Elsevier, Amsterdam.

Engels, S., Bohncke, S.J.P., Bos, J.A.A., Heiri, O., Vandenberghe, J., Wallinga, J., 2008a. Environmental inferences and chironomid-based temperature reconstructions from fragmentary records of the Weichselian Early Glacial and Pleniglacial periods in the Niederlausitz area (eastern Germany). Palaeogeogr. Palaeoclimatol. Palaeoecol. 260, 405–416.

Engels, S., Bohncke, S.J.P., Heiri, O., Schaber, K., Sirocko, F., 2008b. The lacustrine sediment record of Oberwinkler Maar (Eifel, Germany): chironomid and macro-remain-based inferences of environmental changes during Oxygen Isotope Stage 3. Boreas 37, 414–425.

Faegri, K., Iversen, J., 1989. Textbook of Pollen Analysis. John Wiley & Sons, Chichester.

Fairchild, I.J., Baker, A., 2012. Speleothem Science from Process to Past Environments. Wiley-Blackwell A John Wiley & Sons, Ldt.

Felde, V.A., Flantua, S.G.A., Jenks, C.R., Benito, B.M., de Beaulieu, J.-L., Kuneš, P., Magri, D., Nalepka, D., Risebrobakken, B., ter Braak, C.J.F., Allen, J.R.M., Granoszewski, W., Helmens, K.F., Huntley, B., Kondratienė, O., Kalniņa, L., Kupryjanowicz, M., Malkiewicz, M., Milner, A.M., Nita, M., Noryśkiewicz, B., Pidek, I.A., Reille, M., Salonen, J.S., Šeirienė, V., Winter, H., Tzedakis, P.C., Birks, H. J.B., 2020. Compositional turnover and variation in Eemian pollen sequences in Europe. Veg. Hist. Archaeobotany 29, 101–109.

Fletcher, W.J., Sánchez Goñi, M.F., Allen, J.R.M., Cheddadi, R., Combourieu-Nebout, N., Huntley, B., Lawson, I., Londeix, L., Magri, D., Margari, V., Müller, U.C., Naughton, F., Novenko, E., Roucoux, K., Tzedakis, P.C., 2010. Millennial-scale variability during the last glacial in vegetation records from Europe. Quat. Sci. Rev. 29, 2839–2864.

Fohlmeister, J., Schröder-Ritzrau, A., Scholz, D., Spötl, C., Riechelmann, D.F.C., Mudelsee, M., Wackerbarth, A., Gerdes, A., Riechelmann, S., Immenhauser, A., Richter, D.K., Mangini, A., 2012. Bunker Cave stalagmites: an archive for central European Holocene climate variability. Clim. Past 8, 1751–1764.

Fohlmeister, J., Vollweiler, N., Spötl, C., Mangini, A., 2013. COMNISPA II: update of a mid-European isotope climate record, 11 ka to present. Holocene 1–6.

Förster, M.W., Sirocko, F., 2016. The ELSA tephra stack: volcanic activity in the Eifel during the last 500,000 years. Global Planet. Change 142, 100–107.

Förster, M.W., Zemlitskaya, A., Otter, L.M., Buhre, S., Sirocko, F., 2020. Late Pleistocene Eifel eruptions: insights from clinopyroxene and glass geochemistry of tephra layers from Eifel Laminated Sediment Archive sediment cores. J. Quat. Sci. 35, 186–198.

Genty, D., Blamart, D., Ghaleb, B., Plagnes, V., Causse, C., Bakalowicz, M., Zouari, K., Chkir, N., Hellstrom, J., Wainer, K., Bourges, F., 2006. Timing and dynamics of the last deglaciation from European and North African δ13C stalagmite profiles—comparison with Chinese and South Hemisphere stalagmites. Quat. Sci. Rev. 25, 2118–2142.

Genty, D., Blamart, D., Ouahdi, R., Gilmour, M., Baker, A., Jouzel, J., Van-Exter, S., 2003. Precise dating of Dansgaard–Oeschger climate oscillations in western Europe from stalagmite data. Nature 421, 833–837.
Genty, D., Combourieu-Nebout, N., Peyron, O., Blamart, D., Wainer, K., Mansuri, F., Ghaleb, B., Isabello, L., Dormoy, I., von Grafenstein, U., Bonelli, S., Landais, A., Brauer, A., 2010. Isotopic characterization of rapid climatic events during OIS3 and OIS4 in Villars Cave stalagmites (SW-France) and correlation with Atlantic and Mediterranean pollen records. Quat. Sci. Rev. 29, 2799–2820.
Genty, D., Massault, M., Gilmour, M., Baker, A., Verheyden, S., Kepens, E., 1999. Calculation of past dead carbon proportion and variability by the comparison of AMS 14C and tims U/TH ages on two Holocene stalagmites. Radiocarbon 41, 251–270.
Genty, D., Plagnes, V., Causse, C., Cattani, O., Stievenard, M., Falourd, S., Blamart, D., Ouahdi, R., Van-Exter, S., 2002. Fossil water in large stalagmite voids as a tool for paleoprecipitation stable isotope composition reconstitution and paleotemperature calculation. Chem. Geol. 184, 83–95.
Gibert, L., Scott, G.R., Scholz, D., Budsky, A., Ferràndez, C., Ribot, F., Martin, R.A., Lería, M., 2016. Chronology for the cueva victoria fossil site (SE Spain): evidence for early pleistocene afro-iberian dispersals. J. Hum. Evol. 90, 183–197.
Grant, K.M., Rohling, E.J., Ramsey, C.B., Cheng, H., Edwards, R.L., Florindo, F., Heslop, D., Marra, F., Roberts, A.P., Tamisiea, M.E., Williams, F., 2014. Sea-level variability over five glacial cycles. Nat. Commun. 5, 5076.
Hajdas, I., Ascough, P., Garnett, M.H., Fallon, S.J., Pearson, C.L., Quarta, G., Spalding, K. L., Yamaguchi, H., Yoneda, M., 2021. Radiocarbon dating. Nature Reviews Methods Primers 1, 62.
Helmens, K.F., 2014. The Last Interglacial–Glacial cycle (MIS 5–2) re-examined based on long proxy records from central and northern Europe. Quat. Sci. Rev. 86, 115–143.
Helmens, K.F., Engels, S., 2010. Ice-free conditions in eastern Fennoscandia during early Marine Isotope Stage 3: lacustrine records. Boreas 39, 399–409.
Holzkämper, S., Mangini, A., Spötl, C., Mudelsee, M., 2004. Timing and progression of the last interglacial derived from a high alpine stalagmite. Geophys. Res. Lett. 31.
Holzkämper, S., Spötl, C., Mangini, A., 2005. High-precision constraints on timing of Alpine warm periods during the middle to late Pleistocene using speleothem growth periods. Earth Planet Sci. Lett. 236, 751–764.
Kern, O.A., 2021. Percentages of Pollen Data from Late MIS 6 to MIS 1 from Füramoos. Southern Germany. PANGAEA.
Kern, O.A., Koutsodendris, A., Allstädt, F.J., Mächtle, B., Peteet, D.M., Kalaitzidis, S., Christanis, K., Pross, J., 2022. A near-continuous record of climate and ecosystem variability in Central Europe during the past 130 kyrs (Marine Isotope Stages 5–1) from Füramoos, southern Germany. Quat. Sci. Rev. 284, 107505.
Labuhn, I., Genty, D., Vonhof, H., Bourdin, C., Blamart, D., Douville, E., Ruan, J., Cheng, H., Edwards, R.L., Pons-Branchu, E., Pierre, M., 2015. A high-resolution fluid inclusion $\delta^{18}O$ record from a stalagmite in SW France: modern calibration and comparison with multiple proxies. Quat. Sci. Rev. 110, 152–165.
Leyk, H.-J., Lippoldt, H.J., 1997. 40Ar/39Ar-Untersuchungenan spätquatären Vulkanen der Eifel - neue Arbeitsansätze zur Datierung junger Laveströme. Berichte der Deutschen Mineralogischen Gesellschaft, Beiheft zum Europäischen Jahrbuch für Mineralogie 11, 145.
Li, H., Spötl, C., Cheng, H., 2021. A high-resolution speleothem proxy record of the Late Glacial in the European Alps: extending the NALPS19 record until the beginning of the Holocene. J. Quat. Sci. 36, 29–39.
Lisiecki, L.E., Raymo, M.E., 2005. A Pliocene-Pleistocene stack of 57 globally distributed benthic $\delta^{18}O$ records. Paleoceanography 20.
Litt, T., Schölzel, C., Kühl, N., Brauer, A., 2009. Vegetation and climate history in the Westeifel Volcanic Field (Germany) during the past 11 000 years based on annually laminated lacustrine maar sediments. Boreas 38, 679–690.
Ludwig, K.R., 2003. Mathematical-Statistical Treatment of Data and Errors for $^{230}Th/U$ Geochronology, pp. 631–656.
Martrat, B., Grimalt, J.O., Shackleton, N.J., de Abreu, L., Hutterli, M.A., Stocker, T.F., 2007. Four climate cycles of recurring deep and surface water destabilizations on the iberian margin. Science 317, 502–507.
Moseley, G.E., Spötl, C., Brandstätter, S., Erhardt, T., Luetscher, M., Edwards, R.L., 2020. NALPS19: sub-orbital-scale climate variability recorded in northern Alpine speleothems during the last glacial period. Clim. Past 16, 29–50.
Moseley, G.E., Spötl, C., Cheng, H., Boch, R., Min, A., Edwards, R.L., 2015. Termination-II interstadial/stadial climate change recorded in two stalagmites from the north European Alps. Quat. Sci. Rev. 127, 229–239.
Moseley, G.E., Spötl, C., Svensson, A., Cheng, H., Brandstätter, S., Edwards, R.L., 2014. Multi-speleothem record reveals tightly coupled climate between central Europe and Greenland during Marine Isotope Stage 3. Geology 42, 1043–1046.
Niggemann, S., Mangini, A., Richter, D.K., Wurth, G., 2003. A paleoclimate record of the last 17,600 years in stalagmites from the B7 cave, Sauerland, Germany. Quat. Sci. Rev. 22, 555–567.
North Greenland Ice Core Project, m, 2004. High-resolution record of Northern Hemisphere climate extending into the last interglacial period. Nature 431, 147.
Obert, J.C., Scholz, D., Felis, T., Brocas, W.M., Jochum, K.P., Andreae, M.O., 2016. $^{230}Th/U$ dating of Last Interglacial brain corals from Bonaire (southern Caribbean) using bulk and theca wall material. Geochem. Cosmochim. Acta 178, 20–40.
Österreich, G.B.v., 2013. Der Alpenraum zum Höhepunkt der letzten Eiszeit. Geological Survey of Austria, Vienna.
Rahmstorf, S., 2002. Ocean circulation and climate during the past 120,000 years. Nature 419, 207–214.
Rasmussen, S.O., Bigler, M., Blockley, S.P., Blunier, T., Buchardt, S.L., Clausen, H.B., Cvijanovic, I., Dahl-Jensen, D., Johnsen, S.J., Fischer, H., Gkinis, V., Guillevic, M., Hoek, W.Z., Lowe, J.J., Pedro, J.B., Popp, T., Seierstad, I.K., Steffensen, J.P., Svensson, A.M., Vallelonga, P., Vinther, B.M., Walker, M.J.C., Wheatley, J.J., Winstrup, M., 2014. A stratigraphic framework for abrupt climatic changes during the Last Glacial period based on three synchronized Greenland ice-core records: refining and extending the INTIMATE event stratigraphy. Quat. Sci. Rev. 106, 14–28.
Rein, B., Sirocko, F., 2002. In-situ reflectance spectroscopy – analysing techniques for high-resolution pigment logging in sediment cores. Int. J. Earth Sci. 91, 950–954.
Richter, D.K., Dreyer, R., Niggemann, S., Scholz, D., 2018. $^{230}Th/U$-datierte warm- und kaltzeitliche Sinter der Dechenehöhle und die großklimatische Entwicklung der letzten 200.000 Jahre. Mitteilungen des Verbandes der deutschen Höhlen- und Karstforscher 64, 16–24.
Richter, D.K., Goll, K., Grebe, W., Niedermayr, A., Platte, A., Scholz, D., 2015. Weichselzeitliche Kryocalcite als Hinweis für Eisseen in der Hüttenbläserschachthöhle (Iserlohn/NRW). Eiszeitalte & Gegenwart Quaternary Science Journal 64, 67–81.
Riechelmann, D.F.C., Jochum, K.P., Richter, D., Scholz, D., 2023. Mg records of two stalagmites from B7-Cave (northwest Germany) indicating long-term precipitation changes during Early to Mid-Holocene. Int. J. Speleol. 52, 9–22.
Riechelmann, D.F.C., Riechelmann, S., Schröder-Ritzrau, A., 2022. Long-term elemental trends in drip waters from monitoring Bunker Cave: new insights for past precipitation variability. Chem. Geol. 590, 120704.
Riechelmann, D.F.C., Schröder-Ritzrau, A., Scholz, D., Fohlmeister, J., Spötl, C., Richter, D.K., Mangini, A., 2011. Monitoring Bunker Cave (NW Germany): a prerequisite to interpret geochemical proxy data of speleothems from this site. J. Hydrol. 409, 682–695.
Salonen, J.S., Seppä, H., Luoto, M., Bjune, A.E., Birks, H.J.B., 2012. A North European pollen–climate calibration set: analysing the climatic responses of a biological proxy using novel regression tree methods. Quat. Sci. Rev. 45, 95–110.
San-Miguel-Ayanz, J., de Rigo, D., G, C., Houston Durrant, T., Mauri, A., Tinner, W., Ballian, D., Beck, P., Birks, H.J.B., Eaton, E., Enescu, C.M., Pasta, S., Popescu, I., Ravazzi, C., Welk, E., Abad Viñas, R., Azevedo, J.C., Barbati, A., Barredo, J.I., Benham, S.E., Boca, R., Bosco, C., Caldeira, M.C., Cerasoli, S., Chirici, G., Cierjacks, A., Conedera, M., Da Ronch, F., Di Leo, M., García-Viñas, J.I., Gastón González, A., Giannetti, F., Guerrero Hue, N., Guerrero Maldonado, N., López, M.J., Jonsson, R., Krebs, P., Magni, D., Mubareka, S., Mulhern, G., Nieto Quintano, P., Oliveira, S., Pereira, J.S., Pividori, M., Räty, M., Rinaldi, F., Saura, S., Sikkema, R., Sitzia, T., Strona, G., Vidal, C., Vilar, L., Zecchin, B., 2016. European Atlas of Forest Tree Species. Publication Office of the European Union, Luxembourg.
Schaber, K., Sirocko, F., 2005. Lithologie und Stratigraphie der spätpleistozänen Trockenmaare der Eifel. Mainz. Geowiss. Mitt. 33, 295–340.
Scholz, D., Hoffmann, D.L., 2008. $^{230}Th/U$-dating of fossil reef corals and Speleothems. Quatern. Sci. J. (Eiszeitalter und Gegenwart) 57, 52–77.
Sirocko, F., Albert, J., Britzius, S., Dreher, F., Martínez-García, A., Dosseto, A., Burger, J., Terberger, T., Haug, G., 2022. Thresholds for the presence of glacial megafauna in central Europe during the last 60,000 years. Sci. Rep. 12, 20055.
Sirocko, F., Dietrich, S., Veres, D., Grootes, P.M., Schaber-Mohr, K., Seelos, K., Nadeau, M.-J., Kromer, B., Rothacker, L., Röhner, M., Krbetschek, M., Appleby, P., Hambach, U., Rolf, C., Sudo, M., Grim, S., 2013. Multi-proxy dating of Holocene maar lakes and Pleistocene dry maar sediments in the Eifel, Germany. Quat. Sci. Rev. 62, 56–76.
Sirocko, F., Knapp, H., Dreher, F., Förster, M.W., Albert, J., Brunck, H., Veres, D., Dietrich, S., Zech, M., Hambach, U., Röhner, M., Rudert, S., Schwibus, K., Adams, C., Sigl, P., 2016. The ELSA-Vegetation-Stack: reconstruction of Landscape Evolution Zones (LEZ) from laminated Eifel maar sediments of the last 60,000 years. Global Planet. Change 142, 108–135.
Sirocko, F., Krebsbach, F., Albert, J., Britzius, S., Schenk, F.S., Förstel, M.W., in prep. Relation between the central European climate change and the Eifel volcanism during the last 130,000 years: the ELSA-23 Tephra Stack. Quaternary.
Sirocko, F., Martínez-García, A., Mudelsee, M., Albert, J., Britzius, S., Christl, M., Diehl, D., Diensberg, B., Friedrich, R., Fuhrmann, F., Muscheler, R., Hamann, Y., Schneider, R., Schwibus, K., Haug, G.H., 2021. Muted multidecadal climate variability in central Europe during cold stadial periods. Nat. Geosci.
Sirocko, F., Seelos, K., Schaber, K., Rein, B., Dreher, F., Diehl, M., Lehne, R., Jäger, K., Krbetschek, M., Degering, D., 2005. A late Eemian aridity pulse in central Europe during the last glacial inception. Nature 436, 833–836.
Spötl, C., Holzkämper, S., Mangini, A., 2007. The last and the penultimate interglacial as recorded by speleothems from a climatically sensitive high-elevation cave site in the Alps. In: Sirocko, F., Claussen, M., Litt, T., Sánchez-Goñi, M.F. (Eds.), The Climate of Past Interglacials. Elsevier, pp. 471–491.
Spötl, C., Mangini, A., 2002. Stalagmite from the Austrian Alps reveals Dansgaard-Oeschger events during isotope stage 3: implications for the absolute chronology of Greenland ice cores. Earth Planet Sci. Lett. 203, 507–518.
Spötl, C., Mangini, A., 2007. Speleothems and paleoglaciers. Earth Planet Sci. Lett. 254, 323–331.
Spötl, C., Mangini, A., Frank, N., Eichstädter, R., Burns, S.J., 2002. Start of the last interglacial period at 135 ka: evidence from a high Alpine speleothem. Geolog. Soc. Am. 30, 815–818.
Spötl, C., Mangini, A., Richards, D.A., 2006a. Chronology and paleoenviroment of marine isotope stage 3 from two high-elevation speleothems, Austrian Alps. Quat. Sci. Rev. 25, 1127–1136.
Spötl, C., Mangini, A., Richards, D.A., 2006b. Chronology and paleoenvironment of marine isotope stage 3 from two high-elevation speleothems, Austrian Alps. Quat. Sci. Rev. 25, 1127–1136.
Spötl, C., Scholz, D., Mangini, A., 2008. A terrestrial U/Th-dated stable isotope record of the Penultimate Interglacial. Earth Planet Sci. Lett. 276, 283–292.
van den Bogaard, P., Hall, C.M., Schmincke, H.U., York, D., 1989. Precise single-grain $^{40}Ar/^{39}Ar$ dating of a cold to warm climate transition in Central Europe. Nature 342, 523–525.

Wainer, K., Genty, D., Blamart, D., Daëron, M., Bar-Matthews, M., Vonhof, H., Dublyansky, Y., Pons-Branchu, E., Thomas, L., van Calsteren, P., Quinif, Y., Caillon, N., 2011. Speleothem record of the last 180 ka in Villars cave (SW France): Investigation of a large $\delta^{18}O$ shift between MIS6 and MIS5. Quat. Sci. Rev. 30, 130–146.

Wainer, K., Genty, D., Blamart, D., Hoffmann, D., Couchoud, I., 2009. A new stage 3 millennial climatic variability record from a SW France speleothem. Palaeogeogr. Palaeoclimatol. Palaeoecol. 271, 130–139.

Waltgenbach, S., Riechelmann, D.F.C., Spötl, C., Jochum, K.P., Fohlmeister, J., Schröder-Ritzrau, A., Scholz, D., 2021. Climate variability in central Europe during the last 2500 Years reconstructed from four high-resolution multi-proxy speleothem records. Geosciences 11, 166.

Waltgenbach, S., Scholz, D., Spötl, C., Riechelmann, D.F.C., Jochum, K.P., Fohlmeister, J., Schröder-Ritzrau, A., 2020. Climate and structure of the 8.2 ka event reconstructed from three speleothems from Germany. Global Planet. Change 193, 103266.

Wassenburg, J.A., Dietrich, S., Fietzke, J., Fohlmeister, J., Jochum, K.P., Scholz, D., Richter, D.K., Sabaoui, A., Spötl, C., Lohmann, G., Andreae, Meinrat O., Immenhauser, A., 2016. Reorganization of the North Atlantic oscillation during early Holocene deglaciation. Nat. Geosci. 9, 602.

Weber, M., Hinz, Y., Schöne, B.R., Jochum, K.P., Hoffmann, D., Spötl, C., Riechelmann, D.F.C., Scholz, D., 2021. Opposite trends in Holocene speleothem proxy records from two neighboring caves in Germany: a multi-proxy evaluation. Front. Earth Sci. 9.

Weber, M., Scholz, D., Schröder-Ritzrau, A., Deininger, M., Spötl, C., Lugli, F., Mertz-Kraus, R., Jochum, K.P., Fohlmeister, J., Stumpf, C.F., Riechelmann, D.F.C., 2018. Evidence of warm and humid interstadials in central Europe during early MIS 3 revealed by a multi-proxy speleothem record. Quat. Sci. Rev. 200, 276–286.

Woillard, G.M., Mook, W.G., 1982. Carbon-14 dates at Grande pile: correlation of land and sea chronologies. Science 215, 159–161.

Wurth, G., Niggemann, S., Richter, D.K., Mangini, A., 2004. The younger Dryas and Holocene climate record of a stalagmite from Hölloch cave (bavarian Alps, Germany. J. Quat. Sci. 19, 291–298.

Yang, Q., Scholz, D., Jochum, K.P., Hoffmann, D.L., Stoll, B., Weis, U., Schwager, B., Andreae, M.O., 2015. Lead isotope variability in speleothems - a promising new proxy for hydrological change? First results from a stalagmite from western Germany. Chem. Geol. 396, 143–151.

Zöller, L., 1989. Das Alter des Mosenberg-Vulkans in der Vulkaneifel. Die Eifel 84, 415–418.

Zöller, L., Blanchard, H., 2009. The partial heat – longest plateau technique: testing TL dating of Middle and Upper Quaternary volcanic eruptions in the Eifel Area, Germany. E&G Quaternary Sci. J. 58, 86–106.